

Synthesis, radiofluorination and in vivo evaluation of novel fluorinated and iodinated radiotracers for PET imaging and targeted radionuclide therapy of melanoma.

Emilie M.F. Billaud, Latifa Rbah-Vidal, Aurélien Vidal, Sophie Besse, Sébastien Tarrit, Serge Askienazy, Aurélie Maisoniai, Nicole Moins, Jean-Claude Madelmont, Elisabeth Miot-Noirault, Jean-Michel Chezal, and Philippe Auzeloux

J. Med. Chem., **Just Accepted Manuscript** • DOI: 10.1021/jm400877v • Publication Date (Web): 17 Sep 2013

Downloaded from <http://pubs.acs.org> on September 25, 2013

Just Accepted

“Just Accepted” manuscripts have been peer-reviewed and accepted for publication. They are posted online prior to technical editing, formatting for publication and author proofing. The American Chemical Society provides “Just Accepted” as a free service to the research community to expedite the dissemination of scientific material as soon as possible after acceptance. “Just Accepted” manuscripts appear in full in PDF format accompanied by an HTML abstract. “Just Accepted” manuscripts have been fully peer reviewed, but should not be considered the official version of record. They are accessible to all readers and citable by the Digital Object Identifier (DOI®). “Just Accepted” is an optional service offered to authors. Therefore, the “Just Accepted” Web site may not include all articles that will be published in the journal. After a manuscript is technically edited and formatted, it will be removed from the “Just Accepted” Web site and published as an ASAP article. Note that technical editing may introduce minor changes to the manuscript text and/or graphics which could affect content, and all legal disclaimers and ethical guidelines that apply to the journal pertain. ACS cannot be held responsible for errors or consequences arising from the use of information contained in these “Just Accepted” manuscripts.



1
2
3
4
5
6
7
8
9
10
11
12
13
14
15
16
17
18
19
20
21
22
23
24
25
26
27
28
29
30
31
32
33
34
35
36
37
38
39
40
41
42
43
44
45
46
47
48
49
50
51
52
53
54
55
56
57
58
59
60

Synthesis, radiofluorination and *in vivo* evaluation of novel fluorinated and iodinated radiotracers for PET imaging and targeted radionuclide therapy of melanoma.

Emilie M.F. Billaud^a, Latifa Rbah-Vidal^a, Aurélien Vidal^a, Sophie Besse^a, Sébastien Tarrit^a, Serge Askienazy^b, Aurélie Maisonial^a, Nicole Moins^a, Jean-Claude Madelmont^a, Elisabeth Miot-Noirault^a, Jean-Michel Chezal^a and Philippe Auzeloux^{a}.*

^a Clermont Université, Université d'Auvergne, Imagerie Moléculaire et Thérapie Vectorisée, BP 10448, F-63000 Clermont-Ferrand, France. Inserm, U 990, F-63000 Clermont-Ferrand, France.

^b Cyclopharma Laboratories, Biopôle Clermont-Limagne, Saint-Beauzire, F-63360, France.

AUTHOR EMAIL ADDRESS. philippe.auzeloux@inserm.fr

RECEIVED DATE

ABSTRACT.

1
2
3
4 Our project deals with a multimodal approach using a single fluorinated and iodinated melanin-targeting
5
6 structure and offering both imaging (Positron Emission Tomography (PET)/Fluorine-18) and treatment
7
8 (targeted radionuclide therapy/Iodine-131) of melanoma. Six 6-iodoquinoxaline-2-carboxamide
9
10 derivatives with various side chains bearing fluorine were synthesized, radiofluorinated, and their *in*
11
12 *vivo* biodistribution was studied by PET imaging in B16Bl6 primary melanoma-bearing mice. Among
13
14 this series, [¹⁸F]**8** emerged as the most promising compound. [¹⁸F]**8** was obtained by a fully automated
15
16 radiosynthesis process within 57 min with an overall radiochemical yield of 21% decay-corrected. PET
17
18 imaging of [¹⁸F]**8** demonstrated very encouraging results as early as 1 hour post-injection with high
19
20 tumor uptake (14.33±2.11% ID/g), high contrast (11.04±2.87 tumor-to-muscle ratio), and favorable
21
22 clearance properties. These results, associated with the previously reported pharmacokinetic properties
23
24 and dosimetry of **8**, make it a potential agent for both PET imaging and targeted radionuclide therapy of
25
26 melanoma.
27
28
29
30
31
32
33
34
35

36 KEYWORDS. Iodinated and fluorinated radiotracers; Fluorine-18; PET imaging; Biodistribution study;
37
38 Melanoma uptake
39
40
41
42
43
44
45
46
47
48
49
50
51
52
53
54
55
56
57
58
59
60

INTRODUCTION

1
2
3 Malignant melanoma affects more than 150 000 new patients per year worldwide. It accounts for up
4
5 to 90% of all deaths caused by skin cancer and displays a high metastatic potential.¹ Furthermore, this
6
7 disease is the second most common cancer among patients aged 20-39.^{2,3}
8
9

10 Early melanomas (clinical stages I and II, according to the recommendations of the American Joint
11
12 Commission on Cancer) are usually treated with surgical removal of the tumor. Unfortunately, patients
13
14 with highly disseminated melanomas (stages III and IV) have a very poor prognosis, with a median
15
16 survival time of only 6-9 months and a 3-years survival rate of only 10-15%.⁴ These data indicate an
17
18 urgent need to find efficient therapies to treat disseminated melanoma.
19
20

21
22 Standard clinical practice for the initial treatment of cutaneous melanoma involves wide local excision
23
24 of the primary lesion and assessment of metastatic spread to lymph nodes draining the tumor site,
25
26 usually by Sentinel Lymph Node Biopsy (SLNB).^{5,6} Regarding malignant melanoma treatments,
27
28 chemotherapy is mostly ineffective. Monochemotherapy with dacarbazine currently represents the most
29
30 efficient treatment but the obtained response rate remains low (less than 20%) and contributes little to
31
32 overall patient survival.^{7,8} Despite a higher response rate of up to 40% obtained with combination of
33
34 chemotherapeutics or with combination of chemotherapy and cytokines such as interferon or
35
36 interleukin-2, no significant impact on survival has been made in the past 40 years.^{7,9,10,11} Monoclonal
37
38 antibodies anti-CTLA4 (Ipilimumab) and mutated BRAF-V600E inhibitor (Vemurafenib) are two new
39
40 therapeutic strategies that have been tested with significant improvement of survival. However, these
41
42 two treatments induced important side effects including auto-immune response (anti-CTLA4) and
43
44 resistance after initial anti-tumor response (mutated BRAF-V600E inhibitor).^{12,13}
45
46
47
48
49

50 The patient's best opportunity for a cure still remains early diagnosis of disease together with an
51
52 accurate assessment of its metastases. Imaging modalities used for malignant melanoma staging are CT,
53
54 ultrasound, MRI, and PET imaging.¹⁴ Currently, clinical data on PET/CT are solely based on
55
56 [¹⁸F]fluorodeoxyglucose ([¹⁸F]FDG) imaging, but its sensitivity is recognized to be limited for sentinel
57
58 lymph nodes detection. In these cases SLNB, typically performed following intraoperative lymphatic
59
60

mapping, is still the gold standard.^{15,16,17,18} Combination of [¹⁸F]FDG PET imaging and SLNB for evaluation of metastasis can delay definitive management planning and increase the cost of the diagnosis process.⁶ [¹⁸F]FDG PET/CT also fails to highlight micrometastatic lesions that are less than 1 cm in diameter and those located mainly in lungs, liver or brain.¹⁹ Moreover, the use of this non-specific radiotracer may be limited by the risk of false-positives due to abnormal inflammatory areas uptakes for example. Thus, several scintigraphic studies have been developed over the past years, based on tracers related to specific characteristics of melanoma cells.²⁰

Since α -MSH (α -melanocyte-stimulating hormone) receptor MC1R (melanocortin type 1 receptor) is overexpressed in most murine and human melanomas, it has been investigated as a target for selective imaging and therapeutic agents.^{21,22,23} [¹⁸F]Labeled small synthetic peptide [¹⁸F]FB-NAPamide demonstrated that it could differentiate B16/F10 and A375M with high and low MC1R expression respectively, but this tracer showed only moderate tumor uptake and retention.²⁴ Rhenium-cyclized α -MSH analogs have also been studied *in vivo* ([¹⁸F]FB-RMSH-1 and [¹⁸F]FP-RMSH-1) displaying specific, durable and high uptake in MC1R-overexpressing melanoma models.^{25,26}

Different studies demonstrated that melanin pigment, detected in more than 90% of primary melanoma cases, could be a potential target for development of imaging and therapy of melanoma.^{27,28,29} Recently, [¹⁸F]N-[2-(diethylamino)ethyl]-6-fluoro-pyridine-3-carboxamide ([¹⁸F]ICF01006, see Figure 1) exhibited excellent preclinical results as PET tracer for early detection of melanoma lesions in both primary and lung colonies melanoma murine models.^{30,31,32} Moreover, direct comparison with [¹⁸F]FDG showed that [¹⁸F]ICF01006 was superior in terms of contrast and specificity.³² This class of arylcarboxamide compounds with high affinity for melanin-containing cells could also be labeled with high energy radioisotopes (iodine-131 for example) in order to induce an anti-tumoral effect. In previous preclinical studies, a new iodinated quinoxaline-carboxamide derivative ([¹³¹I]ICF01012, [¹³¹I]2, see Figure 1), demonstrated a promising efficacy in a targeted radionuclide therapy (TRT) protocol using murine and human primary melanoma-bearing mice models, with a tumoral concentration primarily correlated to melanin content.^{33,34} Affinity studies of aromatic carboxamide

1 compounds for synthetic melanin revealed the presence of two classes of binding sites, one ionic and the
2 other hydrophobic.²⁸ Secondary ion mass spectrometry (SIMS) analyses also demonstrated a perfect
3 colocalization of ICF01012 with melanosome, illustrating its melanin-specific binding.³³
4
5

6
7 These highly favorable results led us to develop a new multimodal approach, designing iodinated and
8 fluorinated analogs of our lead radiotracer **2**, suitable for both PET imaging (¹⁸F-radiolabeling) and TRT
9 (¹³¹I-radiolabeling) of melanoma.^{35,36} Radiofluorinated molecules were designed to select patients with
10 pigmented melanoma lesions, who may be included in the radionuclide therapy protocol, and to monitor
11 the treatment response.
12
13
14
15
16
17
18

19 Such multimodal concept, with molecules having high affinity for melanin pigment, was first
20 validated with the radiotracer **3** (see Figure 1).³⁷ However the radiolabeling of **3** with ¹⁸F was not
21 transposable to clinical studies due to a two-pot three-step procedure associated with very low
22 radiochemical yields.
23
24
25
26
27

28 With the aim of discovering an appropriate clinical candidate for PET imaging and TRT of
29 melanoma, we designed and synthesized six iodinated and fluorinated analogs of the lead radiotracer
30 **2**.³⁸ All derivatives had in common a 6-iodoquinoxaline-2-carboxamide scaffold and the side chain
31 bearing the fluorine atom on the tertiary amine differed, leading to saturated ethyl (**4**) and propyl (**5**)
32 compounds, alkene (**6**), alkyne (**7**), or pegylated structures (**8** and **9**) (see Figure 2). After radiolabeling
33 with ¹²⁵I, these radiotracers were evaluated *in vivo* in B16 melanoma-bearing mice by γ -scintigraphic
34 imaging: tumoral uptakes were visualized as early as 1 h post injection (p.i.) and up to 10 d p.i., in
35 association with high tumor-to-muscle ratios and a fast clearance of radioactivity from non-target
36 organs. The doses which could be delivered to melanoma tumors ranged from 58.9 to
37 164.8 cGy/injected MBq. These very favorable dosimetry parameters are suitable for efficient targeted
38 radionuclide therapy of disseminated melanoma.³⁸ Based on these promising results, herein we present
39 (i) the syntheses of precursors for ¹⁸F-radiolabeling, (ii) fully automated radiosyntheses with ¹⁸F and (iii)
40 PET imaging of each tracer with tumor uptake evaluation in B16B16 melanoma-bearing mice, compared
41 to *ex vivo* biodistribution study.
42
43
44
45
46
47
48
49
50
51
52
53
54
55
56
57
58
59
60

RESULTS AND DISCUSSION

Chemistry

Radiofluorinations of compounds **5-9** required the syntheses of their corresponding mesylate precursors (Scheme 1). The first three steps of alkyne and alkene mesylate precursors syntheses (**22** and **25** respectively) were common: commercially available 2-butyne-1,4-diol (**10**) was monoprotected using *tert*-butyldimethylsilyl chloride (TBDMSCl) according to a slightly modified protocol developed by Cai *et al.*³⁹ Iodination of the non-protected alcohol function of **11**, in the presence of triphenylphosphine and imidazole, afforded derivative **12**. Subsequently, nucleophilic substitution using phthalimide **13**⁴⁰ and potassium carbonate provided **14** in 41% yield over three steps. This key intermediate was next used in two different synthetic pathways. First, primary amine deprotection using hydrazine monohydrate immediately followed by peptidic coupling with activated ester **19**⁴¹ provided silylated derivative **20**. After deprotection of the alcohol function with tetrabutylammonium fluoride (TBAF), the resulting intermediate **21** was converted into the mesylate precursor **22**, using methanesulfonyl chloride (MsCl), distilled triethylamine as organic base, and catalytic 4-(*N,N*-dimethylamino)pyridine (DMAP) (60 min at rt, 78% yield). Finally, compound **22** was obtained with 44% overall yield from key intermediate **14**. Second, the key alkyne **14** was chemo- and stereoselectively reduced to the corresponding (*E*)-alkene **17**, in a two-step protocol adapted from Trost *et al.*⁴² and Fürstner *et al.*⁴³ Briefly, compound **14** was hydrosilylated with triethoxysilane in the presence of ruthenium complex [Cp**Ru*(MeCN)₃]PF₆ (1.0 mol%) to afford the crude vinylsiloxane intermediate **16**. This hydrosilylation was followed by a protodesilylation under mild conditions with silver(I) fluoride to give selectively (*E*)-alkene **17** in excellent yield (92%). It should be noted that this two-step protocol applied on alkyne **21** did not afford the corresponding alkene **24**. Compound **17** was then subjected to similar protocols than intermediate **14**, *i.e.* deprotection using hydrazine monohydrate immediately followed by peptidic coupling reaction with activated ester **19** to provide silylated derivative **23**. Finally, the deprotection of the alcohol function with TBAF was followed by the conversion of the resulting intermediate **24** into the corresponding mesylate **25**, using MsCl, distilled

1 triethylamine, and DMAP (30 min at rt, 70% yield, see Scheme 2). Compound **25** was obtained with
2
3 60% overall yield from key intermediate **14**.

4
5 Using the same protocol (*i.e.* MsCl, distilled triethylamine and DMAP), mesylate precursors **28**, **29**
6
7 and **31** (see Scheme 2), bearing pegylated (n=3 or n=7) or propyl moiety were obtained in one step in a
8
9 rapid way (60-120 min) with excellent yields (92-95%) from the previously synthesized alcohols **26**, **27**
10
11 and **30**,³⁸ respectively.

12
13
14 It should be noted that due to their limited stability, mesylate precursors **22**, **25** and **31** have to be
15
16 freshly prepared and purified just before radiolabeling with ¹⁸F.

17 18 19 **Radiochemistry**

20
21 Fully automated radiosyntheses of [¹⁸F]**4-9** were performed on a SynChrom R&D module (Raytest).
22
23 For all radiosyntheses, [¹⁸F]F⁻ (Cyclopharma Laboratories) was converted into the dry [¹⁸F]KF₂·K₂₂₂
24
25 complex. Scheme 3 describes radiosyntheses of [¹⁸F]**4-9** and Table 1 summarizes conditions and results
26
27 of all radiochemistry processes.

28
29
30
31 For radiosynthesis of [¹⁸F]**4**, it was not possible to isolate its sulfonate precursor (data not shown) so a
32
33 one-pot two-step procedure involving available stable precursors was chosen. The intermediate [¹⁸F]2-
34
35 fluoroethyl tosylate **33** was obtained by nucleophilic substitution of 1,2-bis(tosyloxy)ethane **32** in
36
37 MeCN.^{44,45} Then, intermediate **33** immediately reacted with the secondary amine function of
38
39 quinoxaline precursor **34**.⁴¹ Best radiochemical yield was obtained with a two-step heating procedure
40
41 (70 °C for 10 min then 110 °C for 10 min). After a semi-preparative HPLC purification, [¹⁸F]**4** was
42
43 manually formulated for biological evaluations: first, the HPLC solvent was evaporated under reduced
44
45 pressure, then the radiolabeled compound was taken up in a saline/EtOH (<5%) solution (formulation
46
47 yield was 97%). Following this procedure, [¹⁸F]**4** was obtained with 11% overall radiochemical yield
48
49 (RCY), a radiochemical purity (RCP) higher than 99% and a 91 min total preparation time.

50
51
52 Regarding the radiosynthesis of [¹⁸F]**5**, the first assay was a similar one-pot two-step procedure
53
54 starting from 1,3-bis(tosyloxy)propane and quinoxaline derivative **34**. In spite of using various reaction
55
56 conditions, a very low radiochemical yields was observed (<2%, data not shown). Thus an easier one-
57
58
59
60

1 step procedure starting from mesylate precursor **31** was successfully carried out. The aliphatic
2 nucleophilic substitution was successfully achieved by heating a solution of **31** in MeCN with
3 anhydrous [¹⁸F]KF, K₂₂₂ complex at 90 °C for 10 min (54% overall RCY, RCP higher than 99% and a
4 total preparation of 70 min).
5
6
7

8
9 Compounds [¹⁸F]**6**, [¹⁸F]**7**, [¹⁸F]**8** and [¹⁸F]**9** were successfully radiolabeled using the same strategy
10 from their corresponding mesylate precursors, **25**, **22**, **28** and **29** respectively. Radiotracers [¹⁸F]**5** and
11 [¹⁸F]**9** were manually formulated for biological evaluations (yields were 91% and 93%, respectively).
12 For [¹⁸F]**6-8** radiotracers, the formulation was fully automated: after dilution in saline of the collected
13 HPLC fraction, the radiolabeled compound was trapped on a C18 cartridge, eluted with EtOH then
14 saline (<10% EtOH in the final solution). Formulation yields were 76-90%. Compounds [¹⁸F]**6-9** were
15 obtained with 16% to 34% overall RCY, RCP higher than 99% and a total preparation time ranging
16 from 57 to 65 min.
17
18
19
20
21
22
23
24
25
26
27

28 **Biological studies**

29 *In vivo* PET imaging

30
31 The preclinical evaluation of [¹⁸F]**4-9** in B16Bl6 primary melanoma-bearing mice by small animal
32 static PET imaging was performed 1 h post tracer injection to compare these tracers. This time point
33 was chosen following a preliminary PET imaging study at 30 min, 1 h, 2 h and 3 h post tracer injection.
34 Results showed that radiotracers were rapidly taken up in target tissues, with a maximal uptake at 1 h
35 p.i. which remained stable up to 3 h p.i. By contrast, activity in non-target tissues such as muscle
36 displayed a fast washout as early as 1 h p.i. (unpublished results). Representative coronal images are
37 shown in Figure 3. For each of the six compounds, tumors were clearly visualized as early as 1 h p.i. For
38 compounds [¹⁸F]**5**, [¹⁸F]**6**, [¹⁸F]**7**, [¹⁸F]**8** and [¹⁸F]**9** significant radioactive signal was also observed in
39 eyes, corroborating the specific uptake in melanin-rich tissues. On the contrary, no significant
40 radioactive signal was observed in eyes for compound [¹⁸F]**4** meaning that tumoral uptake may not be
41 due to specific accumulation. It should be noted that the experiments were performed on the strongly
42 pigmented C57BL/6J mouse model with a high uveal melanin content. Because of murine and human
43
44
45
46
47
48
49
50
51
52
53
54
55
56
57
58
59
60

1 differences in ocular geometry as well as in melanin content, radioactivity uptake in the eyes may not be
2 an issue for clinical transfer.
3

4 For all radiotracers, radioactivity in non-target tissues was mainly located in the abdominal region in
5 accordance with the previously described clearance of this class of compounds *via* urinary and
6 hepatobiliary systems.^{28,37,38} Furthermore, very low radioactivity was detected in non-target organs, such
7 as muscle, brain, heart, and lung, as early as 1 h p.i.
8

9 Highest tumoral uptakes and tumor-to-muscle ratios were obtained for compounds [¹⁸F]**5**, [¹⁸F]**6**,
10 [¹⁸F]**8** and [¹⁸F]**9**. Specific accumulation of radioactivity in B16Bl6 melanoma tumors was 10.56±1.76%
11 ID/g for [¹⁸F]**5**, 6.74±0.73% ID/g for [¹⁸F]**6**, 14.33±2.11% ID/g for [¹⁸F]**8** and 6.63±1.64% ID/g for
12 [¹⁸F]**9**. These values are consistent with our previously published results (10.0±2.8% ID/g for [¹²⁵I]**5**,
13 10.8±2.3% ID/g for [¹²⁵I]**6**, 11.7±2.2% ID/g for [¹²⁵I]**8** and 6.8±1.8% ID/g for [¹²⁵I]**9**).³⁸ Tumor-to-
14 muscle ratio was 11.86±2.43 for [¹⁸F]**5**, 8.27±2.05 for [¹⁸F]**6**, 11.04±2.87 for [¹⁸F]**8** and 6.62±1.90 for
15 [¹⁸F]**9** (Table 2).
16

17 Defluorination and generation of free [¹⁸F]fluoride was negligible for [¹⁸F]**4**, [¹⁸F]**7**, [¹⁸F]**8** and [¹⁸F]**9**
18 at 1 h p.i. as indicated by the low accumulation of radioactivity in the skeleton, whereas significant
19 uptake in bones was observed in PET images performed with [¹⁸F]**5** and [¹⁸F]**6**.
20

21 Based on chemical stability of precursors, tracer accumulation in pigmented tissues and
22 defluorination, compounds [¹⁸F]**8** and [¹⁸F]**9** seemed to be the most relevant and promising radiotracers
23 for melanoma PET imaging. Compared to our previously described multimodal radiotracer [¹⁸F]**3**,³⁷ a
24 higher melanoma uptake was observed with [¹⁸F]**8** (12.72±4.45% ID/g vs. 8.30±1.70% ID/g, at 2 h p.i.;
25 p=0.038). Compared to [¹⁸F]**1**, which is currently one of the best melanin-targeting PET radiotracers,
26 [¹⁸F]**8** demonstrated a similar tumoral uptake in the same experimental model (14.33±2.11% ID/g vs.
27 11.44±2.67% ID/g for [¹⁸F]**1** at 1 h p.i.; p=0.18) and a nearly 2-fold greater tumor-to-muscle ratio
28 (11.04±2.87 vs. 6.40±1.73 for [¹⁸F]**1** at 1 h p.i.; p=0.020).^{31,32}
29

30 *Ex vivo* biodistribution

31
32
33
34
35
36
37
38
39
40
41
42
43
44
45
46
47
48
49
50
51
52
53
54
55
56
57
58
59
60

Selected compounds [^{18}F]**8** and [^{18}F]**9** were studied by *ex vivo* biodistribution experiments by direct-sampling tumors and tissues of interest at 1 h, 2 h and 3 h post tracer injection (Table 3). Uptakes in pigmented tissues were similar to those obtained by PET imaging at 1 h p.i. and remained high and stable until 3 h p.i. for both molecules (*i.e.* tumoral uptake at 3 h p.i. was $11.55\pm 1.24\%$ ID/g for [^{18}F]**8** and $6.76\pm 1.35\%$ ID/g for [^{18}F]**9**). Furthermore, a significantly higher tumoral uptake was observed for [^{18}F]**8** compared to [^{18}F]**9**, at all time points ($p=0.035$, $p=0.0016$ and $p=0.0001$ at 1 h, 2 h and 3 h p.i. respectively). Very low tracers accumulation in muscle and blood led to higher tumor-to-muscle and tumor-to-blood ratios reaching values of 14.46 ± 3.06 ($p=0.0007$) and 14.43 ± 1.75 ($p=0.0005$) respectively for [^{18}F]**8** and values of 6.64 ± 2.69 and 5.27 ± 0.20 respectively for [^{18}F]**9** at 3 h p.i. Low bone accumulation was observed at 1 h p.i. ($1.40\pm 0.10\%$ ID/g for [^{18}F]**8** and $1.82\pm 0.55\%$ ID/g for [^{18}F]**9**). Partial *in vivo* defluorination of [^{18}F]**8** and [^{18}F]**9** occurred at 3 h p.i., which were not correlated with *in vitro* stability in saline (RCP >99% for at least 6 h). Regarding radiotracer elimination, [^{18}F]**9** demonstrated a significantly higher accumulation in intestine compared to [^{18}F]**8** ($p=0.018$, $p=0.0000001$ and $p=0.02$ at 1 h, 2 h and 3 h p.i. respectively), suggesting that despite a higher hydrophilicity of [^{18}F]**9** (LogD = 0.95 ± 0.02 vs 1.52 ± 0.03 for [^{18}F]**8**), renal excretion of this tracer was not favored. Hence, [^{18}F]**8** derivative, bearing a triethylene glycol side chain, appeared more attractive than compound [^{18}F]**9** bearing an heptaethylene glycol side chain.

[^{18}F]**8** stability study.

In tumor and eyes (melanin-containing tissues), more than 99% of the radioactive signal corresponded to unchanged [^{18}F]**8**, at 1 h and 2 h p.i. (Table 4). On the contrary, a fast breakdown of [^{18}F]**8** was observed in blood (15% of unchanged [^{18}F]**8** at 30 min) and liver (8% of unchanged [^{18}F]**8** at 1 h). In urine samples, less than 1% of unchanged radiotracer was detected. These results demonstrated that once linked to melanin in pigmented tissues, [^{18}F]**8** remained unchanged, whereas important and fast metabolic processes occurred in non-specific tissues.

CONCLUSION

1 In summary, six [^{18}F]fluorinated 6-iodoquinoxaline-2-carboxamide derivatives with various side
2 chains were synthesized and evaluated. [^{18}F]4-9 were radiosynthesized on an automated module in good
3 yields, high radiochemical purity and displayed excellent chemical stability in physiological serum.
4
5

6
7 Biodistribution studies by *in vivo* PET imaging in B16Bl6 primary melanoma-bearing mice
8 demonstrated that four compounds out of six exhibited a high tropism for pigmented melanoma and also
9 high tumor-to-background ratios as early as 1 h p.i. Regarding PET imaging results and *in vivo* stability,
10 the two best candidates [^{18}F]8 and [^{18}F]9 were then investigated in an *ex vivo* biodistribution study in
11 B16Bl6-bearing mice. This study confirmed that derivative [^{18}F]8 had the highest tumoral uptake in this
12 model and exhibited excellent pharmacokinetic features. It displayed lower uptake and faster clearance
13 of radioactivity from non-target organs, with hepatobiliary/renal excretion pathways, resulting in higher
14 tumor-to-blood and tumor-to-muscle ratios than for [^{18}F]9.
15
16

17 Thus, [^{18}F]8 exhibited high tumoral uptake and favorable kinetics leading to highly contrasted images
18 as early as 1 h p.i. This work demonstrated that in terms of chemistry, radiochemistry and *in vivo*
19 biodistribution, radiotracer [^{18}F]8 appears suitable for PET imaging.
20
21

22 Besides, as previously reported, [^{125}I]8 showed high tumoral uptakes up to five days p.i. in the same
23 melanoma-bearing mice model (12.4±2.3% ID/g, 8.6±3.6% ID/g, 5.8±2.4% ID/g at 24 h, 72 h, 5 d p.i.
24 respectively), and a high calculated tumoral dosimetry (103.5 cGy/MBq for [^{131}I]8).³⁸ These results
25 make this compound a promising agent for targeted radionuclide therapy of melanoma (assay in
26 progress).
27
28

29 In conclusion, in our multimodality approach, radiotracer 8 appears as a good candidate for both
30 imaging (PET/Fluorine-18) and treatment (TRT/Iodine-131) of melanoma.
31
32

33 **EXPERIMENTAL SECTION**

34 **Materials and General Methods**

35
36 *Chemistry.* All reagents and solvents were purchased from the following commercial suppliers:
37 Sigma-Aldrich, Acros Organics, ThermoFischer, Alfa Aesar, TCI Europe, Carlo Erba, SDS. All
38
39
40
41
42
43
44
45
46
47
48
49
50
51
52
53
54
55
56
57
58
59
60

1 solvents were dried using common techniques.⁴⁶ Unless otherwise noted, moisture sensitive reactions
2 were conducted under dry argon atmosphere. Thin layer chromatography (TLC) was performed on silica
3 gel 60 F₂₅₄ plates or neutral aluminium oxide 60 F₂₅₄ plates (Merck or SDS) and visualized with UV
4 light and/or developed with iodine, ninhydrin or potassium permanganate. Flash chromatography was
5 performed on silica gel 60A normal phase, 35–70 μm (SDS). Florisil was purchased at Sigma Aldrich
6 (Fluka). Uncorrected melting points (mp) were recorded on Reichert-Jung-Koffler apparatus. NMR
7 spectra (200 MHz for ¹H and 50 MHz for ¹³C) were recorded on a Bruker Avance 200 instrument; ¹⁹F
8 NMR spectra (470 MHz) were recorded on a Bruker DRX 500 apparatus using tetrafluorotoluene as
9 internal reference (δ: –63.7 ppm). δ were expressed in ppm. Infrared spectra (IR) were recorded on a
10 FTIR Nicolet Impact 410, a FT Vector 22 or a Nicolet IS10 with attenuated total reflectance (ATR)
11 accessory. Electron impact mode mass spectra (EI-MS) were obtained on a HP5890 series II
12 chromatograph coupled to HP5985B mass spectrometer. The analysis of samples was performed in
13 MeCN at a final concentration of 1 pmol.μL⁻¹. Electrospray ionization mass spectra (ESI-MS) were
14 recorded on a Esquire-LC (Bruker Daltonics, Wissenbourg, France) spectrometer. The analysis of
15 samples was performed in MeCN at a final concentration of 1 pmol.μL⁻¹. Microanalyses were
16 performed by Analytical Laboratory of the CNRS (Vernaison, France) for the elements indicated.

17
18
19
20
21
22
23
24
25
26
27
28
29
30
31
32
33
34
35
36
37
38 *Radiochemistry.* No-carrier-added fluorine-18 (half-life: 109.8 min) was produced via the [¹⁸O(p,
39 n)¹⁸F] nuclear reaction by irradiation of a 2.8 mL [¹⁸O]water target (>97%-enriched, Bruce Technology,
40 Chapel Hill, USA) on a CPH14 cyclotron (14 MeV proton Beam, Cyclopharma laboratories, Saint-
41 Beuzire, France). Typical production of [¹⁸F]fluoride at the end of bombardment for a 90 to 100 μA.h
42 (120 min) irradiation: 185 GBq (5 Ci). Radiochemistry syntheses and semi-preparatives HPLC were
43 performed using a mono-reactor Synchron R&D synthesis module (Raytest, Straubenhardt, Germany).
44 Semi-preparative HPLC were conducted on a Waters Symmetry Semi-Prep C18 column (300x7.8 mm;
45 porosity: 7 μm) or Waters Spherisorb Semi-Prep SiO₂ column (250x10 mm, porosity 10 μm); flow rate:
46 3.0 mL.min⁻¹; temperature: rt; absorbance detection at λ = 254 nm. Radio-TLCs were run on Merck pre-
47 coated neutral aluminium oxide 60 F₂₅₄ plates with a mixture of DCM and EtOH as solvents (98:2, v/v).
48
49
50
51
52
53
54
55
56
57
58
59
60

1 Detection of K_{222} was achieved using the standard chloroplatinate color test.⁴⁷ Radioactivity
2 measurements were performed on a gamma counter equipped with a NaI(Tl) well type scintillation
3 counter (Model 1480 Wizard, Perkin Elmer Life Sciences, Boston, USA). Analytical HPLC were
4 performed on a PerkinElmer Series 200 equipped with a multi-wavelength UV Diode Array Detector
5 (DAD) and a GABI Star gamma-detector (Raytest, Straubenhardt, Germany) at a flow rate of 0.9 or
6 1.0 mL.min⁻¹. Column: Waters Symmetry C18 (150x4.6 mm; porosity: 5 μ m) or Waters Spherisorb
7 SiO₂ (150x4.6 mm, porosity 5 μ m); temperature: rt; absorbance detection at $\lambda = 254$ nm. Purity and
8 specific activity were determined by analytical HPLC. For each tested compound, purity was >99%.
9 The identity of each [¹⁸F]fluorinated compound was confirmed by coelution with its non-radioactive
10 counterpart. A delay time of 0.35 min was observed between the first detector (UV) and the second
11 (gamma).
12
13
14
15
16
17
18
19
20
21
22
23
24
25

26 *Octanol-water distribution coefficient (LogD)*. Approximately 74 kBq of radiotracer was added to a
27 mixture of PBS (pH 7.4, 1.0 mL) and octanol (1.0 mL) in an Eppendorf microcentrifuge tube. The
28 mixture was vigorously vortexed for 1 min, three times at rt. After centrifugation (3,000 rpm, 5 min),
29 aliquots (100 μ L) of both layers were sampled and the radioactivity was measured using the gamma
30 counter. Three independent experiments were performed in duplicates.
31
32
33
34
35
36
37

38 *Cell culture*. The B16Bl6 syngenic melanoma cells were obtained from Dr Fidler Laboratories (Texas
39 University, Houston, USA). Cells cultures were maintained as monolayers in Dulbecco's modified
40 Eagle's medium (DMEM)/Glutamax(Invitrogen, Cergy Pontoise, France) supplemented with 10% calf
41 serum (Sigma, Saint Quentin, Fallavier, France), 1% vitamins (Invitrogen), 1 mM sodium pyruvate
42 (Invitrogen), 1% non-essential amino acids (Invitrogen) and 4 μ g.mL⁻¹ of gentamycin base (Invitrogen).
43 The cells were grown at 37 °C in a humidified incubator containing 5% CO₂.
44
45
46
47
48
49
50
51

52 *Primary murine melanoma model*. Animals were handled and cared in accordance with the guidelines
53 for the Care and Use of Laboratory Animals (National Research Council, 1996) and European Directive
54 86/609/EEC. Protocols were performed under the authorization of the French Direction des Services
55 Vétérinaires (authorization no. CE 86-12) and conducted under the supervision of authorized
56
57
58
59
60

1 investigators in accordance with the institution's recommendations for the use of laboratory animals.
2 C57BL/6J male mice (6-8 weeks old) were obtained from Charles River (l'Arbresle, France). Cells in
3 exponential growth phase were trypsinized, washed with phosphate buffer saline (PBS), and
4 resuspended in PBS. Mice anesthetized by isoflurane (2%) inhalation were inoculated with 3×10^5
5 melanoma B16Bl6 cells in PBS (0.1 mL) by subcutaneous injection on the right shoulder.
6
7
8
9
10

11 *In vivo PET imaging.* PET imaging sessions were performed at day-10 or day-14 after inoculation
12 (tumoral volume range of $431.8 \pm 154.3 \text{ mm}^3$). Whole-body PET scans were acquired 1 h after
13 intravenous injection of [^{18}F]labeled compound (9-12 MBq/0.15 mL) via the tail vein (range 2-8
14 animals/compound) and were anesthetized by intraperitoneal administration (200 μL /20 g-mouse) of a
15 mixture of ketamine (Imalgene 500, Rhône Mérieux, Lyon, France) and xylazine (Rompun, Bayer,
16 France) in saline, 4:1 ratio. Whole-body acquisition (25 min-duration) was performed using a small-
17 animal PET device (eXplore Vista, GE Healthcare) with a 250-700 keV energy window set and 6 ns
18 coincidence-timing window. The spatial resolution of this system was 1.4 mm Full Width at Half
19 Maximum at the center of the Field Of View.⁴⁸ Images were reconstructed using a 2D ordered-subset
20 expectation maximization (Fore/2D OSEM) method including corrections for scanner dead time, scatter
21 radiations and randoms. No corrections were applied for partial volume or attenuation.
22
23
24
25
26
27
28
29
30
31
32
33
34
35
36
37

38 Regional radiotracer uptake was quantified by standard Region-Of-Interest (ROI) analysis with
39 eXplore Vista software package (GE Healthcare) as previously described.³² Briefly, on decay-corrected
40 whole-body coronal images, a manual 2D-ROI was drawn around the whole tumor and different organs.
41 The reference tissue ROI was drawn on caudal thigh muscle and considered as background. The mean
42 counts per pixel per minute were obtained from the ROI and converted to counts per milliliter per min
43 using a calibration constant. By assuming a tissue density of 1 g.mL^{-1} , the ROIs were converted to
44 counts/g/min. An ROI-derived % ID/g of tissue was then determined by dividing counts per gram per
45 minute by injected dose. *In vivo* tumor-to-background ratio was calculated by dividing the % ID/g value
46 of tumor by the % ID/g value of muscle.
47
48
49
50
51
52
53
54
55
56
57
58
59
60

1 *Ex vivo biodistribution studies.* *Ex vivo* biodistribution study was performed for [¹⁸F]**8** and [¹⁸F]**9**.
2
3 Experiments were undertaken at day-10 or day-14 after cells implantation (n=3-6 animals/group).
4
5 Animals were sacrificed by CO₂ asphyxiation 1 h, 2 h and 3 after i.v. injection of [¹⁸F]labeled
6
7 compound (9-12 MBq). Tumors, major organs and tissues were promptly excised, harvested, weighted
8
9 and their radioactivity counted. After radioactive decay correction, results were expressed as % ID/g.
10

11 [¹⁸F]**8** stability study. Six primary melanoma-bearing mice were injected with [¹⁸F]**8** (18 MBq/i.v.)
12
13 and sacrificed 30 min, 1 h and 2 h p.i. To determine the metabolic stability of [¹⁸F]**8**, blood, liver, urine,
14
15 eyes and tumor samples were collected. Blood was immediately centrifuged for 5 min at 3,000 rpm and
16
17 plasma directly investigated by analytical HPLC. Urine sample was collected in the bladder and directly
18
19 investigated by analytical HPLC. Tumors, eyes and livers were pooled, suspended in MeOH/NH₄OH
20
21 99.8:0.2 (5 mL), homogenized using GentleMACS dissociator (Miltenyi Biotec, Bergisch Gladbach,
22
23 Germany) and centrifuged for 5 min at 3,000 rpm. The extraction efficiency was determined by
24
25 measuring the radioactivity of supernatants and precipitates (extraction yields: 61%, 55% and 99%
26
27 respectively). Supernatants were passed through a 0.22 μm Millipore filter and then concentrated to a
28
29 volume between 200 and 500 μL before injection (duplicate) onto the analytical HPLC (C18 column;
30
31 MeOH/H₂O/NH₄OH 0:99.8:0.2 to 29.9:69.9:0.2 v/v/v linear gradient in 8 min then 29.9:69.9:0.2 to
32
33 59.9:39.9:0.2 linear gradient in 1 min then 59.9:39.9:0.2 to 89.9:9.9:0.2 linear gradient in 8 min then
34
35 0:99.8:0.2 isocratic during 8 min; 0.9 mL.min⁻¹).
36
37
38
39
40
41
42

43 *Statistical Analysis.* Quantitative data are expressed as mean ± standard deviation (SD). Means were
44
45 compared using Student t test. Values were considered statistically significant for p<0.05.
46
47
48

49 Chemistry

50 *N*-[2-[*N*-Ethyl-*N*-(2-fluoroethyl)amino]ethyl]-6-iodoquinoxaline-2-carboxamide **4**. Fluorine-19
51
52 standard compound **4** was prepared as described by Maisonial, Billaud *et al.*³⁸ *R*_f (Al₂O₃, DCM/EtOH,
53
54 98:2, v/v) 0.72; IR (CCl₄) ν 1474, 1522, 1685, 2855, 2927 cm⁻¹; ¹H NMR (CDCl₃) δ 1.12 (t, 3H, *J* =
55
56 7.1 Hz), 2.75 (q, 2H, *J* = 7.1 Hz), 2.87 (t, 1H, *J* = 6.0 Hz), 2.92 (dt, 2H, ³*J*_{H-F} = 26.8 Hz, *J* = 5.0 Hz),
57
58
59
60

3.62 (q, 2H, $J = 6.0$ Hz), 4.58 (dt, 2H, $^2J_{\text{H-F}} = 47.7$ Hz, $J = 5.0$ Hz), 7.81 (d, 1H, $J = 8.8$ Hz), 8.05 (dd, 1H, $J = 8.8, 1.8$ Hz), 8.45 (br, 1H), 8.58 (d, 1H, $J = 1.8$ Hz), 9.62 (s, 1H); ^{13}C NMR (CDCl_3) δ 11.8, 37.3, 48.5, 52.9, 53.6 (d, $^2J_{\text{C-F}} = 20$ Hz), 82.5 (d, $^1J_{\text{C-F}} = 167$ Hz), 98.0, 130.9, 138.6, 139.6, 139.7, 144.0, 144.4, 144.6, 163.1; ^{19}F NMR (CDCl_3) δ -220.22; MS m/z 416 (M^+ , 1), 104 (100), 76 (12), 56 (8).

N-[2-[*N*-Ethyl-*N*-(3-fluoropropyl)amino]ethyl]-6-iodoquinoxaline-2-carboxamide **5**. Fluorine-19 standard compound **5** was prepared as described by Maisonial, Billaud *et al.*³⁸ R_f (SiO_2 , ethyl acetate) 0.36; ^1H NMR (CD_3CN) δ 1.05 (t, 3H, $J = 7.1$ Hz), 1.82 (m, 2H), 2.64 (m, 6H), 3.52 (q, 2H, $J = 5.9$ Hz), 4.56 (dt, 2H, $^2J_{\text{H-F}} = 47.4$ Hz, $J = 6.0$ Hz), 7.87 (d, 1H, $J = 8.8$ Hz), 8.08 (dd, 1H, $J = 8.8, 1.9$ Hz), 8.41 (br, 1H), 8.60 (d, 1H, $J = 1.9$ Hz), 9.63 (s, 1H); ^{13}C NMR (CD_3CN) δ 11.5, 28.1 (d, $^4J_{\text{C-F}} = 1$ Hz), 37.3, 47.7, 52.3, 52.9 (d, $^3J_{\text{C-F}} = 11$ Hz), 82.7 (d, $^1J_{\text{C-F}} = 166$ Hz), 98.2, 131.0, 138.6, 139.5, 139.8, 143.8, 144.4, 144.6, 162.2; ^{19}F NMR (CD_3CN) δ -220.47; ESI-MS m/z [$\text{M}+\text{H}$] $^+$ 431.10.

N-[2-[*N*-Ethyl-*N*-[(*E*)-4-fluorobut-2-enyl]amino]ethyl]-6-iodoquinoxaline-2-carboxamide **6**. Fluorine-19 standard compound **6** was prepared as described by Maisonial, Billaud *et al.*³⁸ R_f (Al_2O_3 , DCM/EtOH , 99:1, v/v) 0.36; mp 50-52 °C; IR (CCl_4) ν 1160, 1353, 1475, 1520, 1682, 2817, 2850-3000, 3409 cm^{-1} ; ^1H NMR (CDCl_3) δ 1.08 (t, 3H, $J = 7.1$ Hz), 2.63 (q, 2H, $J = 7.1$ Hz), 2.72 (t, 2H, $J = 6.2$ Hz), 3.21 (m, 2H), 3.57 (q, 2H, $J = 5.9$ Hz), 4.81 (dd, 2H, $^2J_{\text{H-F}} = 47.0$ Hz, $J = 4.3$ Hz), 5.90 (m, 2H), 7.81 (d, 1H, $J = 8.8$ Hz), 8.07 (dd, 1H, $J = 8.8, 1.8$ Hz), 8.32 (m, 1H), 8.59 (d, 1H, $J = 1.8$ Hz), 9.63 (s, 1H); ^{13}C NMR (CDCl_3) δ 12.2, 37.4, 47.8, 51.9, 55.2 (d, $^4J_{\text{C-F}} = 1$ Hz), 83.0 (d, $^1J_{\text{C-F}} = 162$ Hz), 98.1, 127.4 (d, $^2J_{\text{C-F}} = 17$ Hz), 130.9, 133.2 (d, $^3J_{\text{C-F}} = 12$ Hz), 138.7, 139.7, 139.8, 144.1, 144.5, 144.7, 163.0; ^{19}F NMR (CDCl_3) δ -211.13 (t, $^2J_{\text{H-F}} = 48.2$ Hz); ESI-MS m/z [$\text{M}+\text{H}$] $^+$ 442.90.

N-[2-[*N*-Ethyl-*N*-(4-fluorobut-2-ynyl)amino]ethyl]-6-iodoquinoxaline-2-carboxamide **7**. Fluorine-19 standard compound **7** was prepared as described by Maisonial, Billaud *et al.*³⁸ R_f (Al_2O_3 , DCM/EtOH , 99:1, v/v) 0.86; IR (CCl_4) ν 1475, 1522, 1685, 2928 cm^{-1} ; ^1H NMR (acetone-d_6) δ 1.11 (t, 3H, $J = 7.2$ Hz), 2.64 (q, 2H, $J = 7.2$ Hz), 2.80 (t, 2H, $J = 6.1$ Hz), 3.59 (m, 4H), 4.97 (dt, 2H, $^2J_{\text{H-F}} = 47.5$ Hz, $J = 1.7$ Hz), 7.80 (d, 1H, $J = 8.8$ Hz), 8.05 (dd, 1H, $J = 8.8, 1.8$ Hz), 8.25 (br, 1H), 8.58 (d, 1H, $J = 1.8$ Hz), 9.62 (s, 1H); ^{13}C NMR (acetone-d_6) δ 12.9, 37.7, 42.2 (d, $^4J_{\text{C-F}} = 3$ Hz), 48.3, 52.9, 71.5 (d,

$^1J_{C-F} = 161$ Hz), 80.3 (d, $^2J_{C-F} = 22$ Hz), 85.5 (d, $^3J_{C-F} = 12$ Hz), 98.3, 131.8, 139.1, 140.2, 140.5, 145.0, 145.3, 145.5, 163.5; ^{19}F NMR (acetone- d_6) δ -213.79; ESI-MS m/z $[M+H]^+$ 441.10.

N-(12-ethyl-1-fluoro-3,6,9-trioxa-12-azatetradecan-14-yl)-6-iodoquinoxaline-2-carboxamide **8**.

Fluorine-19 standard compound **8** was prepared as described by Maisonial, Billaud *et al.*³⁸ R_f (SiO₂, ethyl acetate/EtOH, 85:15, v/v) 0.30; IR (ATR diamond accessory) ν 1046, 1107, 1352, 1473, 1523, 1592, 1669, 2868, 2916, 3300-3400 cm^{-1} ; 1H NMR (CDCl₃) δ 1.07 (t, 3H, $J = 7.1$ Hz), 2.65 (q, 2H, $J = 7.1$ Hz), 2.77 (m, 4H), 3.61 (m, 12H), 3.69 (m, 2H), 4.53 (dt, 2H, $^2J_{H-F} = 47.7$ Hz, $J = 4.1$ Hz), 7.81 (d, 1H, $J = 8.8$ Hz), 8.07 (dd, 1H, $J = 8.8, 1.8$ Hz), 8.42 (br, 1H), 8.60 (d, 1H, $J = 1.8$ Hz), 9.63 (s, 1H); ^{13}C NMR (CDCl₃) δ 11.5, 37.1, 48.9, 52.8 (2C), 70.8 (6C), 83.2 ($^1J_{C-F} = 169$ Hz), 98.1, 131.0, 138.6, 139.5, 139.7, 144.1, 144.4, 144.7, 163.3; ^{19}F NMR (CDCl₃) δ -223.1; ESI-MS m/z $[M+H]^+$ 549.20.

N-(24-ethyl-1-fluoro-3,6,9,12,15,18,21-hepta-oxa-24-aza-hexacosan-26-yl)-6-iodoquinoxaline-2-carboxamide **9**. Fluorine-19 standard compound **9** was prepared as described by Maisonial, Billaud *et al.*³⁸ R_f (SiO₂, ethyl acetate/EtOH, 5:5, v/v containing 0.5% of NH₄OH) 0.32; IR (ATR diamond accessory) ν 1129, 1353, 1474, 1527, 1593, 1675, 2800-3000, 3300-3400 cm^{-1} ; 1H NMR (CDCl₃) δ 1.07 (t, 3H, $J = 7.1$ Hz), 2.67 (q, 2H, $J = 7.1$ Hz), 2.79 (m, 4H), 3.61 (m, 30H), 4.55 (dt, 2H, $^2J_{H-F} = 47.8$ Hz, $J = 4.1$ Hz), 7.83 (d, 1H, $J = 8.8$ Hz), 8.08 (dd, 1H, $J = 8.8, 1.6$ Hz), 8.46 (br, 1H), 8.61 (d, 1H, $J = 1.6$ Hz), 9.64 (s, 1H); ^{13}C NMR (CDCl₃) δ 11.5, 37.0, 48.0, 52.9, 53.0, 70.6 (14C), 83.3 (d, $^1J_{C-F} = 163$ Hz), 98.1, 131.0, 138.6, 139.7, 139.7, 144.1, 144.4, 144.7, 163.3; ^{19}F NMR (CDCl₃) δ -223.2; ESI-MS m/z $[M+H]^+$ 725.20.

4-(*tert*-butyldimethylsilyloxy)but-2-yn-1-ol (**II**). To a solution of 2-butyne-1,4-diol **10** (10.0 g, 116 mmol) in anhydrous *N,N*-dimethylformamide (DMF) (125 mL) were added successively, imidazole (5.9 g, 87.1 mmol) and TBDMSCl (10.5 g, 69.7 mmol). The mixture was stirred at rt for 24 h. The reaction was quenched with MeOH (40 mL) and water (120 mL) and then extracted with ethyl acetate (3 x 200 mL). The organic layers were combined, washed with brine (200 mL), dried on MgSO₄, filtered and evaporated under reduced pressure. The residue was taken up in ethyl acetate (200 mL) and washed with water (3 x 200 mL). The organic layer was dried on MgSO₄, filtered and evaporated under

1 reduced pressure. The crude product was purified by chromatography (SiO₂, DCM/EtOH, 98:2, v/v) to
2 give compound **11** (9.45 g, 47.2 mmol) as a yellow oil. Yield 68%; *R_f* (SiO₂, DCM/EtOH, 98:2, v/v)
3 0.35; IR (NaCl) ν 778, 837, 1084, 1256, 1472, 2350, 2859, 2930, 3200–3500 cm⁻¹. ¹H NMR (CDCl₃) δ
4 0.09 (s, 6H), 0.87 (s, 9H), 2.93 (br, 1H), 4.25 (s, 2H), 4.31 (s, 2H). ¹³C NMR (CDCl₃) δ -5.1 (2C), 18.4,
5 25.9 (3C), 51.2, 51.8, 83.1, 84.4. EI-MS *m/z* 185 (<1) 143 (3), 126 (3), 125 (28), 85 (5), 77 (6), 76 (8),
6 75 (100), 73 (7), 61 (3), 59 (3), 57 (3).

7
8
9
10
11
12
13
14 *tert-butyl(4-iodobut-2-ynyloxy)dimethylsilane (12)*. To a solution of alcohol **11** (9.35 g, 46.7 mmol)
15 vigorously stirred at 0 °C in anhydrous DCM (250 mL) were added successively, imidazole (4.13 g,
16 60.7 mmol), triphenylphosphine (15.9 g, 60.7 mmol) and iodine (15.4 g, 60.7 mmol). The mixture was
17 stirred at 0 °C for 30 min and allowed to stand at rt for 1 h before addition of an aqueous solution of
18 10% sodium bisulfite (320 mL). After decanting, the aqueous layer was extracted with DCM (3 x
19 150 mL). The organic layers were combined, dried on MgSO₄, filtered and evaporated under reduced
20 pressure. The residue containing the desired product was triturated in *n*-pentane (280 mL) and stirred for
21 45 min. The precipitate was filtered and washed with *n*-pentane (50 mL). The filtrate was evaporated
22 under reduced pressure and the crude product was purified by chromatography (SiO₂, *n*-pentane/diethyl
23 ether, 99:1, v/v) to give compound **12** (11.2 g, 36.1 mmol) as a pale yellow oil. Yield 78%; *R_f* (SiO₂, *n*-
24 pentane/diethyl ether, 99:1, v/v) 0.30; IR (NaCl) ν 778, 837, 1086, 1255, 1471, 2350, 2857, 2929 cm⁻¹.
25 ¹H NMR (CDCl₃) δ 0.11 (s, 6H), 0.89 (s, 9H), 3.71 (m, 2H), 4.31 (m, 2H). ¹³C NMR (CDCl₃) δ -18.5, -
26 5.1 (2C), 18.4, 25.9 (3C), 51.9, 81.6, 84.0.

27
28
29
30
31
32
33
34
35
36
37
38
39
40
41
42
43
44
45 *N*-[2-[*N*-[4-(*tert*-butyldimethylsilyloxy)but-2-ynyl]-*N*-ethylamino]ethyl]phthalimide (**14**). To a
46 solution of 2-[2-(ethylamino)ethyl]-1*H*-phthalimide hydrochloride **13** (4.51 g, 17.7 mmol)⁴⁰ in
47 anhydrous MeCN (85 mL) were successively added potassium carbonate (2.45 g, 17.7 mmol) and
48 compound **12** (5.50 g, 17.7 mmol). The mixture was stirred at rt for 72 h. Saturated aqueous sodium
49 carbonate solution (250 mL) was added, and the aqueous layer was extracted with DCM (3 x 150 mL).
50 The organic layers were combined, dried on MgSO₄, filtered and evaporated under reduced pressure.
51 The obtained residue was purified by chromatography (SiO₂, DCM/EtOH, 8:2, v/v) to give compound
52
53
54
55
56
57
58
59
60

1 **14** (5.54 g, 13.8 mmol) as an orange solid. Yield 78%; R_f (SiO₂, DCM/EtOH, 8:2, v/v) 0.85; mp 49–
2 51 °C. IR (NaCl) ν 777, 837, 1032, 1254, 1335, 1401, 1431, 1470, 1706, 2273, 2858, 2929 cm⁻¹. ¹H
3 NMR (CDCl₃) δ 0.10 (s, 6H), 0.88 (s, 9H), 0.96 (t, 3H, $J = 7.1$ Hz), 2.56 (q, 2H, $J = 7.1$ Hz), 2.79 (t, 2H,
4 $J = 6.4$ Hz), 3.51 (s, 2H), 3.78 (t, 2H, $J = 6.4$ Hz), 4.31 (t, 2H, $J = 1.7$ Hz), 7.70 (m, 2H), 7.80 (m, 2H).
5 ¹³C NMR (CDCl₃) δ -5.0 (2C), 12.8, 18.4, 25.9 (3C), 35.9, 41.8, 47.6, 50.8, 51.8, 79.4, 83.9, 123.3 (2C),
6 132.3 (2C), 133.9 (2C), 168.5 (2C). ESI-MS m/z [M + H]⁺ 401.26.

7
8
9
10
11
12
13
14 *N*-[4-(*tert*-butyldimethylsilyloxy)but-2-ynyl]-*N*-ethyl-1,2-ethylenediamine (**15**). To a solution of
15 phthalimide **14** (5.54 g, 13.8 mmol) in EtOH (500 mL) was added hydrazine monohydrate (6.71 mL,
16 138 mmol, 10 equiv). The mixture was stirred at rt for 17 h. After cooling to 0 °C for 4 h, the precipitate
17 was filtered and washed with EtOH (50 mL). The filtrate was evaporated under reduced pressure and
18 taken up in cold EtOH (50 mL), filtered and washed with cold EtOH (50 mL). Last steps were repeated
19 until no more white solid appeared after evaporation of the filtrate. Compound **15** (3.74 g, 13.8 mmol)
20 was obtained as a yellow oil and used without further purification. Yield quant.; R_f (Al₂O₃, DCM/EtOH,
21 8:2, v/v) 0.23; IR (ATR diamond accessory) ν 837, 1116, 1255, 1472, 1641, 2275, 2858, 2931 cm⁻¹. ¹H
22 NMR (CDCl₃) δ 0.11 (s, 6H), 0.90 (s, 9H), 1.05 (t, 3H, $J = 7.1$ Hz), 2.59 (q, 2H, $J = 7.1$ Hz), 2.71 (t, 2H,
23 $J = 5.5$ Hz), 3.23 (m, 2H), 3.44 (s, 2H), 4.32 (s, 2H). ¹³C NMR (CDCl₃) δ -5.0 (2C), 12.8, 18.4, 25.9
24 (3C), 37.9, 41.5, 47.5, 51.8, 52.4, 79.1, 84.0.

25
26
27
28
29
30
31
32
33
34
35
36
37
38
39
40
41 *N*-[2-[*N*-[(*E*)-4-(*tert*-butyldimethylsilyloxy)but-2-enyl]-*N*-ethylamino]ethyl]phthalimide (**17**). This
42 protocol was adapted from Trost *et al.*⁴² and Fürstner *et al.*⁴³ To a solution of phthalimide **14** (525 mg,
43 1.31 mmol) in anhydrous DCM (8 mL) were successively added at 0 °C, triethoxysilane (290 μ L,
44 1.57 mmol) and catalyst [Cp**Ru*(MeCN)₃]PF₆ (7.0 mg, 13.1 μ mol). The mixture was stirred at 0 °C for
45 10 min and then at rt for 2 h. Diethyl ether was added (25 mL), and the mixture was filtered on a Florisil
46 pad (100-200 mesh). The pad was washed with diethyl ether (50 mL), DCM (25 mL), and then the
47 filtrate was evaporated under reduced pressure. The obtained residue (710 mg, 1.26 mmol) was taken up
48 in tetrahydrofuran (THF) (11 mL), and a suspension of silver fluoride 1M in MeOH (2.5 mL,
49 2.51 mmol) was added. The mixture was stirred at rt in darkness for 2.5 h, filtered and then washed with
50
51
52
53
54
55
56
57
58
59
60

1 ether (20 mL) and ethyl acetate (20 mL). The filtrate was evaporated under reduced pressure. The
2 obtained residue was purified by chromatography (SiO₂, ethyl acetate/cyclohexane, 3:7, v/v) to give
3 compound **17** (485 mg, 1.21 mmol) as a pale yellow oil. Yield 92%; *R_f* (SiO₂, ethyl
4 acetate/cyclohexane, 3:7, v/v) 0.25; IR (ATR diamond accessory) ν 778, 839, 1101, 1257, 1396, 1469,
5 1718, 2856, 2930 cm⁻¹. ¹H NMR (500 MHz, CDCl₃) δ 0.07 (s, 6H), 0.89 (s, 9H), 0.97 (t, 3H, *J* =
6 7.1 Hz), 2.56 (q, 2H, *J* = 7.1 Hz), 2.71 (t, 2H, *J* = 6.8 Hz), 3.14 (d, 2H, *J* = 5.9 Hz), 3.76 (t, 2H, *J* =
7 6.8 Hz), 4.11 (d, 2H, *J* = 4.7 Hz), 5.61 (dt, 1H, *J* = 15.5, 5.9 Hz), 5.66 (dt, 1H, *J* = 15.5, 4.7 Hz), 7.70
8 (m, 2H), 7.83 (m, 2H). ¹³C NMR (CDCl₃) δ -5.1 (2C), 12.1, 18.4, 26.0 (3C), 36.1, 47.4, 50.5, 55.3, 63.6,
9 123.2 (2C), 127.4, 132.3 (2C), 132.5, 133.9 (2C), 168.5 (2C). ESI-MS *m/z* [M + H]⁺ 403.32.

10
11
12
13
14
15
16
17
18
19
20
21
22 *N*-[*(E)*-4-(*tert*-butyldimethylsilyloxy)but-2-enyl]-*N*-ethyl-1,2-ethylenediamine (**18**). Compound **18** was
23 prepared following the same procedure described above for **15**, starting from phthalimide **17** (250 mg,
24 0.62 mmol). Compound **18** (169 mg, 0.62 mmol) was obtained as a pale yellow oil and used without
25 further purification. Yield quant.; *R_f* (SiO₂, ethyl acetate/cyclohexane, 1:1, v/v) 0.12; ¹H NMR
26 (CDCl₃) δ 0.05 (s, 6H), 0.90 (s, 9H), 0.99 (t, 3H, *J* = 7.1 Hz), 2.50 (m, 4H), 2.60 (br, 2H), 2.73 (t, 2H, *J*
27 = 6.1 Hz), 3.07 (m, 2H), 4.13 (m, 2H), 5.67 (m, 2H). ¹³C NMR (CDCl₃) δ -5.1(2C), 11.9, 18.6, 26.0
28 (3C), 39.6, 47.6, 55.4, 55.8, 63.6, 127.6, 132.3.

29
30
31
32
33
34
35
36
37
38 *N*-[2-[[*N*-Ethyl-*N*-(4-(*tert*-butyldimethylsilyloxy)but-2-ynyl)]amino]ethyl]-6-iodoquinoxaline-2-
39
40 *carboxamide* (**20**). To a suspension of activated ester 4-nitrophenyl 6-iodoquinoxaline-2-carboxylate **19**
41 (1.00 g, 2.38 mmol) in anhydrous THF (10 mL) was added a solution of compound **15** (0.71 g,
42 2.61 mmol) in anhydrous THF (15 mL). The mixture was stirred at rt for 18 h. The solvent was
43 evaporated under reduced pressure, the residue was taken up in DCM (25 mL) and the mixture was
44 poured into a 1M aqueous NaOH solution (75 mL). The aqueous layer was extracted with DCM
45 (3 x 25 mL), the combined organic layers were washed with a 5% aqueous sodium carbonate solution
46 (2 x 75 mL), dried on MgSO₄, filtered and evaporated under reduced pressure. The obtained residue was
47 purified by chromatography (SiO₂, ethyl acetate/*n*-pentane, 9:1, v/v) to give compound **20** (820 mg,
48 1.48 mmol) as a yellow gum. Yield 63%; *R_f* (SiO₂, ethyl acetate/*n*-pentane, 9:1, v/v) 0.42; IR (NaCl) ν
49
50
51
52
53
54
55
56
57
58
59
60

407, 777, 836, 1074, 1253, 1353, 1387, 1472, 1472, 1518, 1593, 1656, 1683, 2273, 2858, 2929, 3363 cm⁻¹. ¹H NMR (CDCl₃) δ 0.08 (s, 6H), 0.82 (s, 9H), 1.04 (t, 3H, *J* = 7.1 Hz), 2.57 (q, 2H, *J* = 7.1 Hz), 2.74 (t, 2H, *J* = 5.9 Hz), 3.46 (br, 2H), 3.53 (q, 2H, *J* = 5.9 Hz), 4.27 (br, 2H), 7.72 (d, 1H, *J* = 8.9 Hz), 7.94 (dd, 1H, *J* = 8.9, 1.8 Hz), 8.22 (m, 1H), 8.47 (d, 1H, *J* = 1.8 Hz), 9.54 (s, 1H). ¹³C NMR (CDCl₃) δ -5.1 (2C), 13.0, 18.3, 25.8 (3C), 37.1, 41.7, 47.6, 51.8, 51.9, 79.4, 83.9, 98.0, 130.8, 138.5, 139.4, 139.6, 144.0, 144.3, 144.6, 162.9. ESI-MS *m/z* [M + H]⁺ 553.17.

N-[2-[[*N*-Ethyl-*N*-(4-hydroxybut-2-ynyl)]amino]ethyl]-6-iodoquinoxaline-2-carboxamide (**21**). To a solution of protected alcohol **20** (200 mg, 0.36 mmol) in THF (6 mL) was added a 1M solution of TBAF in THF (543 μL, 0.54 mmol). The mixture was stirred at rt for 2 h. The reaction was quenched by addition of a saturated aqueous sodium hydrogencarbonate solution (60 mL), followed by distilled water (30 mL) and then ethyl acetate (30 mL). The mixture was extracted with ethyl acetate (3 x 30 mL). The organic layers were combined, washed with brine (30 mL), dried on MgSO₄, filtered and evaporated under reduced pressure. The obtained residue was purified by chromatography (SiO₂, ethyl acetate) to give compound **21** (140 mg, 0.32 mmol) as a yellow solid. Yield 89%; *R*_f (SiO₂, ethyl acetate) 0.17; mp 119–121 °C. IR (NaCl) ν 407, 1022, 1353, 1473, 1523, 1592, 1664, 2273, 2865, 2925, 3200–3600 cm⁻¹. ¹H NMR (CDCl₃) δ 1.10 (t, 3H, *J* = 7.1 Hz), 2.62 (q, 2H, *J* = 7.1 Hz), 2.74 (t, 2H, *J* = 6.1 Hz), 3.52 (br, 2H), 3.60 (q, 2H, *J* = 6.1 Hz), 4.29 (t, 2H, *J* = 1.8 Hz), 7.81 (d, 1H, *J* = 8.9 Hz), 8.03 (dd, 1H, *J* = 8.9, 1.8 Hz), 8.29 (m, 1H), 8.57 (d, 1H, *J* = 1.7 Hz), 9.61 (s, 1H). ¹³C NMR (CDCl₃) δ 12.9, 37.3, 42.0, 48.0, 51.0, 52.0, 80.2, 83.9, 98.2, 130.8, 138.6, 139.5, 139.8, 143.9, 144.4, 144.6, 163.1. ESI-MS *m/z* [M + H]⁺ 439.09.

N-[2-[[*N*-Ethyl-*N*-[(*E*)-4-(*tert*-butyldimethylsilyloxy)but-2-enyl)]amino]ethyl]-6-iodoquinoxaline-2-carboxamide (**23**). Compound **23** was prepared following the same procedure described above for **20**, using compound **18** (147 mg, 0.54 mmol). Protected alcohol **23** (180 mg, 0.32 mmol) was obtained as a yellow oil. Yield 93%; *R*_f (SiO₂, ethyl acetate) 0.43; IR (ATR diamond accessory) ν 778, 838, 1102, 1257, 1354, 1386, 1473, 1525, 1593, 1683, 2855, 2929, 3300–3400 cm⁻¹. ¹H NMR (CDCl₃) δ 0.00 (s, 6H), 0.83 (s, 9H), 1.05 (t, 3H, *J* = 7.1 Hz), 2.56 (q, 2H, *J* = 7.1 Hz), 2.70 (t, 2H, *J* = 6.0 Hz), 3.16 (br,

1
2
3
4
5
6
7
8
9
10
11
12
13
14
15
16
17
18
19
20
21
22
23
24
25
26
27
28
29
30
31
32
33
34
35
36
37
38
39
40
41
42
43
44
45
46
47
48
49
50
51
52
53
54
55
56
57
58
59
60

2H), 3.56 (q, 2H, $J = 6.0$ Hz), 4.11 (br, 2H), 5.72 (m, 2H), 7.79 (d, 1H, $J = 8.8$ Hz), 8.03 (dd, 1H, $J = 8.8, 1.8$ Hz), 8.35 (m, 1H), 8.57 (d, 1H, $J = 1.8$ Hz), 9.61 (s, 1H). ^{13}C NMR (CDCl_3) δ -5.2 (2C), 12.2, 18.4, 26.0 (3C), 37.3, 47.5, 51.6, 55.3, 63.5, 97.9, 127.3, 130.9, 132.6, 138.6, 139.6 (2C), 144.1, 144.4, 144.7, 162.9. ESI-MS m/z $[\text{M} + \text{H}]^+$ 555.21.

N-[2-[*N*-Ethyl-*N*-[(*E*)-4-hydroxybut-2-enyl]amino]ethyl]-6-iodoquinoxaline-2-carboxamide (24).

Compound **24** was prepared following the same procedure described above for **21**, starting from **23** (171 mg, 0.31 mmol). Alcohol **24** (135 mg, 0.31 mmol) was obtained as a yellow oil. Yield 99%; R_f (SiO_2 , DCM/EtOH, 9:1, v/v) 0.20; IR (ATR diamond accessory) ν 978, 1355, 1475, 1533, 1593, 1675, 2823, 2934, 3200–3500 cm^{-1} . ^1H NMR (500 MHz, CDCl_3) δ 1.08 (t, 3H, $J = 7.1$ Hz), 2.63 (q, 2H, $J = 7.1$ Hz), 2.73 (t, 2H, $J = 6.2$ Hz), 3.18 (d, 2H, $J = 6.1$ Hz), 3.56 (q, 2H, $J = 6.2$ Hz), 4.10 (d, 2H, $J = 5.2$ Hz), 5.77 (dt, 1H, $J = 15.5, 6.1$ Hz), 5.86 (dt, 1H, $J = 15.5, 5.2$ Hz), 7.81 (d, 1H, $J = 8.8$ Hz), 8.04 (dd, 1H, $J = 1.6, 8.8$ Hz), 8.33 (m, 1H), 8.57 (d, 1H, $J = 1.6$ Hz), 9.60 (s, 1H). ^{13}C NMR (CDCl_3) δ 12.1, 37.5, 48.1, 51.6, 55.6, 63.2, 98.1, 128.8, 130.8, 132.7, 138.6, 139.6, 139.8, 144.0, 144.4, 144.6, 163.1. ESI-MS m/z $[\text{M} + \text{H}]^+$ 441.13.

General Procedure: Syntheses of mesylates 22, 25, 28, 29 and 31. To a solution of the corresponding alcohol, distilled triethylamine (1.2 equiv) and DMAP (0.1 equiv) in anhydrous DCM (1-2 mL) was added MsCl (1.2 equiv). The mixture was stirred at rt for 30-120 min and then poured into a saturated aqueous sodium hydrogencarbonate solution (10-30 mL). After decanting, the aqueous layer was extracted with ethyl acetate (3 x 15 mL). The organic layers were combined, washed with brine (15 mL), dried on MgSO_4 , filtered and evaporated under reduced pressure to afford the crude product.

N-[2-[*N*-Ethyl-*N*-(4-methanesulfonyloxybut-2-ynyl)]amino]ethyl]-6-iodoquinoxaline-2-carboxamide (22). The alcohol **21** (25 mg, 57 μmol) was treated according to the general method described above (reaction time: 60 min) and purified by chromatography (SiO_2 , ethyl acetate) to give compound **22** (23 mg, 45 μmol) as a yellow gum. Yield 78%; R_f (SiO_2 , ethyl acetate) 0.31; IR (NaCl) ν 732, 907, 1025, 1177, 1370, 1474, 1523, 1674, 2254, 2869, 2928, 3200-3600. ^1H NMR (CDCl_3) δ 1.12 (t, 3H, $J = 7.1$ Hz), 2.64 (q, 2H, $J = 7.1$ Hz), 2.81 (t, 2H, $J = 6.1$ Hz), 3.10 (s, 3H), 3.59 (s, 2H), 3.62 (q, 2H, $J =$

6.1 Hz), 4.88 (t, 2H, $J = 1.8$ Hz), 7.81 (d, 1H, $J = 8.9$ Hz), 8.07 (dd, 1H, $J = 8.9, 1.9$ Hz), 8.25 (m, 1H), 8.59 (d, 1H, $J = 1.9$ Hz), 9.62 (s, 1H). ^{13}C NMR (CDCl_3) δ 12.9, 37.0, 38.9, 41.8, 47.9, 52.1, 57.6, 80.2, 83.9, 98.2, 130.8, 138.7, 139.5 (2C), 139.8, 143.9 (2C), 144.4 (2C), 144.7, 163.1. ESI-MS m/z $[\text{M} + \text{H}]^+$ 517.04.

N-[2-[*N*-Ethyl-*N*-[(*E*)-4-methanesulfonyloxybut-2-enyl]amino]ethyl]-6-iodoquinoxaline-2-carboxamide (**25**). The alcohol **24** (25.5 mg, 58 μmol) was treated according to the general method described above (reaction time: 30 min) and purified by chromatography (SiO_2 , ethyl acetate) to give compound **25** (21 mg, 41 μmol) as a yellow gum. Yield 70%; R_f (SiO_2 , ethyl acetate) 0.35; IR (NaCl) ν 409, 828, 927, 1172, 1352, 1474, 1527, 1592, 1670, 2858, 2929, 3300–3400 cm^{-1} . ^1H NMR (CDCl_3) δ 1.09 (t, 3H, $J = 7.1$ Hz), 2.63 (q, 2H, $J = 7.1$ Hz), 2.73 (t, 2H, $J = 6.1$ Hz), 2.99 (s, 3H), 3.21 (m, 2H), 3.58 (q, 2H, $J = 6.1$ Hz), 4.69 (m, 2H), 5.88 (m, 2H), 7.84 (d, 1H, $J = 8.9$ Hz), 8.09 (dd, 1H, $J = 8.9, 1.7$ Hz), 8.36 (m, 1H), 8.61 (d, 1H, $J = 1.7$ Hz), 9.64 (s, 1H). ^{13}C NMR (CDCl_3) δ 12.1, 37.3, 38.1, 47.8, 51.8, 54.9, 69.8, 98.0, 127.3, 130.9, 132.6, 138.6, 139.8, 144.7, 162.9. ESI-MS m/z $[\text{M} + \text{H}]^+$ 519.07

N-(12-ethyl-1-methanesulfonyloxy-3,6,9-trioxa-12-azatetradecan-14-yl)-6-iodoquinoxaline-2-carboxamide (**28**). The alcohol **26** (80 mg, 146 μmol , prepared as described by Maisonial, Billaud *et al.*³⁸) was treated according to the general method described above (reaction time: 60 min) and purified by chromatography (SiO_2 , DCM \rightarrow DCM/EtOH, 9:1, v/v) to give compound **28** (85 mg, 136 μmol) as a yellow gum. Yield 93%; R_f (SiO_2 , DCM/EtOH, 9:1, v/v) 0.37; IR (ATR diamond accessory) ν 751, 917, 1106, 1171, 1349, 1473, 1592, 1525, 1668, 2849, 2916, 3300–3400 cm^{-1} . ^1H NMR (CDCl_3) δ 1.12 (t, 3H, $J = 7.1$ Hz), 2.85 (m, 6H), 3.06 (s, 3H), 3.60 (m, 12H), 3.73 (m, 2H), 4.36 (m, 2H), 7.83 (d, 1H, $J = 8.8$ Hz), 8.06 (dd, 1H, $J = 8.8, 1.8$ Hz), 8.53 (m, 1H), 8.60 (d, 1H, $J = 1.8$ Hz), 9.62 (s, 1H). ^{13}C NMR (CDCl_3) δ 11.7, 37.2, 37.8, 48.9, 52.9, 53.0, 69.1, 69.3, 70.5 (5C), 98.1, 130.9, 138.6, 139.6, 139.8, 144.1, 144.4, 144.7, 163.2. ESI-MS m/z $[\text{M} + \text{H}]^+$ 625.25.

N-(24-ethyl-1-methanesulfonyloxy-3,6,9,12,15,18,21-hepta-oxa-24-azahexacosan-26-yl)-6-iodoquinoxaline-2-carboxamide (**29**). The alcohol **27** (91 mg, 126 μmol , prepared as described by Maisonial, Billaud *et al.*³⁸) was treated according to the general method described above (reaction time:

120 min) and purified by chromatography (SiO₂, DCM → DCM/EtOH, 9:1, v/v) to give compound **29** (95 mg, 119 μmol) as a yellow gum. Yield 95%; *R_f* (SiO₂, DCM/EtOH, 8:2, v/v) 0.50; IR (ATR diamond accessory) ν 733, 923, 1128, 1176, 1354, 1474, 1593, 1527, 1675, 2800-3000, 3300-3400 cm⁻¹. ¹H NMR (CDCl₃) δ 1.04 (t, 3H, *J* = 7.1 Hz), 2.64 (q, 2H, *J* = 7.1 Hz), 2.73 (m, 4H), 3.06 (s, 3H), 3.61 (m, 28H), 3.73 (t, 2H, *J* = 4.5 Hz), 4.35 (t, 2H, *J* = 4.5 Hz), 7.80 (d, 1H, *J* = 8.8 Hz), 8.05 (dd, 1H, *J* = 8.8, 1.3 Hz), 8.41 (m, 1H), 8.57 (d, 1H, *J* = 1.3 Hz), 9.61 (s, 1H). ¹³C NMR (CDCl₃) δ 12.2, 37.6, 37.8, 48.7, 52.9, 53.0, 69.1, 69.4, 70.2-70.6 (13C), 98.0, 130.9, 138.6, 139.6, 139.7, 144.2, 144.4, 144.7, 163.0. ESI-MS *m/z* [M + H]⁺ 801.33.

N-[2-[*N*-Ethyl-*N*-(3-methanesulfonyloxypropyl)amino]ethyl]-6-iodoquinoxaline-2-carboxamide (**31**).

The alcohol **30** (30 mg, 70 μmol, prepared as described by Maisonial, Billaud *et al.*³⁸) was treated according to the general method described above (reaction time: 60 min) and purified by chromatography (SiO₂, DCM → DCM/EtOH, 9:1, v/v) to give compound **31** (32.5 mg, 64 μmol) as a yellow gum. Yield 92%; *R_f* (SiO₂, DCM/EtOH, 9/1, v/v) 0.43; ¹H NMR (CDCl₃) δ 1.07 (t, 3H, *J* = 7.1 Hz), 1.91 (quint., 2H, *J* = 6.4 Hz), 2.65 (m, 6H), 2.97 (s, 3H), 3.58 (q, 2H, *J* = 5.9 Hz), 4.37 (t, 2H, *J* = 6.2 Hz), 7.86 (d, 1H, *J* = 8.9 Hz), 8.08 (dd, 1H, *J* = 8.9, 1.9 Hz), 8.32 (m, 1H), 8.60 (d, 1H, *J* = 1.9 Hz), 9.62 (s, 1H). ¹³C NMR (CDCl₃) δ 11.8, 27.3, 37.3, 37.5, 47.4, 49.2, 52.3, 67.9, 98.2, 131.0, 138.4, 139.6, 139.8, 144.0, 144.5, 144.6, 163.0. ESI-MS *m/z* [M + H]⁺ 507.08.

Radiochemistry

[¹⁸F]KF, K₂₂₂ complex. The activated [¹⁸F]KF, K₂₂₂ complex was obtained by usual method in 19 min. Briefly, the aqueous [¹⁸F]F⁻ solution from target was flushed through an anion exchange resin (Sep-Pak Light Accell Plus QMA cartridge, Waters). The radioactivity was eluted to the reactor with a K₂CO₃ (3.0 mg) and Kryptofix (K₂₂₂, 15.0 mg) solution (1 mL, MeCN/H₂O, 70:30, v/v). Solvents were evaporated under reduced pressure and under a gentle stream of helium at 110 °C for 10 min. A second azeotropic drying was repeated by addition of anhydrous MeCN (1.0 mL).

[¹⁸F]N-[2-[N-Ethyl-N-(2-fluoroethyl)amino]ethyl]-6-iodoquinoxaline-2-carboxamide [¹⁸F]4. To the dry [¹⁸F]KF,K₂₂₂ complex were added a solution of ditosylate compound **32** in dry MeCN (6 mg/0.5 mL) and a solution of amine **34** in dry MeCN (12 mg/1.0 mL).⁴¹ The mixture was heated at 70 °C for 10 min and then at 110 °C for 10 min. After cooling to rt, the reaction mixture was diluted with DCM (2 mL) and directly purified by semi-preparative HPLC (Semi-Prep SiO₂ column; DCM/EtOH 98:02 v/v; *t_R* = 14.9 min). The solvent was evaporated under reduced pressure and the formulation was achieved in EtOH/saline (1:9 v/v; formulation yield = 97%). [¹⁸F]4 was obtained in 91 min with 11% overall RCY (6% non-decay-corrected). RCP was determined by analytical HPLC (SiO₂ column; DCM/EtOH 98:2 v/v; 1 mL.min⁻¹; *t_R*=12.65 min) and was >99%. Radiotracer was radiochemically stable at rt for at least 6 h after preparation.

[¹⁸F]N-[2-[N-Ethyl-N-(3-fluoropropyl)amino]ethyl]-6-iodoquinoxaline-2-carboxamide [¹⁸F]5. To the dry [¹⁸F]KF,K₂₂₂ complex was added a solution of mesylate precursor **31** in dry MeCN (14 mg/1 mL) and the mixture was heated at 90 °C for 10 min. After cooling to rt, the reaction mixture was diluted with HPLC eluent (2.5 mL) and purified by semi-preparative HPLC (Semi-Prep SiO₂ column; DCM/EtOH/NH₄OH 93.8:6:0.2 v/v/v; *t_R* = 9.4 min). The solvent was evaporated under reduced pressure and the formulation was achieved in EtOH/saline (1:9 v/v; formulation yield = 91%). [¹⁸F]5 was obtained in 70 min with 54% overall RCY (34% non-decay-corrected). RCP was determined by analytical HPLC (SiO₂ column; DCM/EtOH/NH₄OH 99.8:0:0.2 to 89.8:10:0.2 in 10 min; 1 mL.min⁻¹; *t_R* = 8.67 min) and was >99%. Radiotracer was radiochemically stable at rt for at least 6 h after preparation. LogD = 1.28±0.04.

[¹⁸F]N-[2-[N-Ethyl-N-[(E)-4-fluorobut-2-enyl]amino]ethyl]-6-iodoquinoxaline-2-carboxamide [¹⁸F]6. To the dry [¹⁸F]KF,K₂₂₂ complex was added a solution of mesylate precursor **25** in dry MeCN (12 mg/1 mL) and the mixture was heated at 90 °C for 10 min. After cooling to rt, the reaction mixture was diluted with HPLC eluent (2.5 mL) and purified by semi-preparative HPLC (Semi-Prep C18 column; MeOH/H₂O/NH₄OH 74.9:24.9:0.2 v/v/v; *t_R* = 16.0 min). The collected solution was diluted in saline (20 mL) then passed through a C18 cartridge (Sep-Pak Plus C18, Waters). The cartridge was then

1 washed with water (5 mL) before being eluted with EtOH (1 mL) and then saline (10 mL). The solution
2 was finally passed through a Millipore filter (0.22 μm) and collected in a sterile vial (formulation yield:
3 83%). [^{18}F]6 was obtained in 62 min with 16% overall RCY (11% non-decay-corrected). RCP was
4 determined by analytical HPLC (C18 column; MeOH/H₂O/NH₄OH 74.9:24.9:0.2 v/v/v; 1 mL.min⁻¹; t_{R}
5 = 8.62 min) and was >99%. Radiotracer was radiochemically stable at rt for at least 6 h after
6 preparation. LogD = 1.64±0.02.
7
8
9
10
11
12

13
14 [^{18}F]N-[2-[[N-Ethyl-N-(4-fluorobut-2-ynyl)]amino]ethyl]-6-iodoquinoxaline-2-carboxamide [^{18}F]7.
15

16 To the dry [^{18}F]KF,K₂₂₂ complex was added a solution of mesylate precursor **22** in dry MeCN
17 (10 mg/1 mL) and the mixture was heated at 90 °C for 10 min. After cooling to rt, the reaction mixture
18 was diluted with HPLC eluent (2.5 mL) and purified by semi-preparative HPLC (Semi-Prep C18
19 column; MeOH/H₂O/NH₄OH (74.9:24.9:0.2 v/v/v; t_{R} = 11.2 min). The collected solution was diluted
20 with saline (20 mL) then passed through a C18 cartridge (Sep-Pak Plus C18, Waters). The cartridge was
21 then washed with water (5 mL) before being eluted with EtOH (700 μL) and then saline (10 mL). The
22 solution was finally passed through a Millipore filter (0.22 μm) and collected in a sterile vial
23 (formulation yield: 76%). [^{18}F]7 was obtained in 59 min with 22% overall RCY (15% non-decay-
24 corrected). RCP was determined by analytical HPLC (C18 column; MeOH/H₂O/NH₄OH 74.9:24.9:0.2
25 v/v/v; 1 mL.min⁻¹; t_{R} = 8.33 min) and was >99%. Radiotracer was radiochemically stable at rt for at
26 least 6 h after preparation. LogD = 1.90±0.02.
27
28
29
30
31
32
33
34
35
36
37
38
39
40
41

42 [^{18}F]N-(12-ethyl-1-fluoro-3,6,9-trioxa-12-azatetradecan-14-yl)-6-iodoquinoxaline-2-carboxamide
43

44 [^{18}F]8. To the dry [^{18}F]KF,K₂₂₂ complex was added a solution of mesylate precursor **28** in dry MeCN
45 (13 mg/1 mL) and the mixture was heated at 90 °C for 10 min. After cooling to rt, the reaction mixture
46 was diluted with HPLC eluent (2.5 mL) and purified by semi-preparative HPLC (C18 column;
47 MeOH/H₂O/NH₄OH (74.7:24.9:0.4 v/v/v; t_{R} = 12.5 min). The collected solution was diluted with saline
48 (20 mL) then passed through a C18 cartridge (Sep-Pak Plus C18, Waters). The cartridge was then
49 washed with water (5 mL) before being eluted with EtOH (900 μL) and then saline (8 mL). The solution
50 was collected in a sterile vial (formulation yield: 90%). [^{18}F]8 was obtained in 57 min with 21% overall
51
52
53
54
55
56
57
58
59
60

1 RCY (14% non-decay-corrected) and a specific activity of 45-53 GBq.μmol⁻¹. RCP was determined by
2 analytical HPLC (C18 column; MeOH/H₂O/NH₄OH v/v/v; 59.9:39.9:0.2 to 89.8:10:0.2 linear gradient
3 in 10 min then 59.9:39.9:0.2 isocratic during 7 min; 0.9 mL.min⁻¹; t_R = 12.51 min) and was >99%. Color
4 spot test showed no detection of K₂₂₂ in the final injectable [¹⁸F]**8** solution. Radiotracer was
5 radiochemically stable at rt for at least 22 h after preparation. LogD = 1.52±0.03.
6
7

8 [¹⁸F]N-(24-ethyl-1-fluoro-3,6,9,12,15,18,21-hepta-oxa-24-aza-hexacosan-26-yl)-6-iodoquinoxaline-2-
9 carboxamide [¹⁸F]**9**. To the dry [¹⁸F]KF₂.K₂₂₂ complex was added a solution of mesylate precursor **29** in
10 dry MeCN (15 mg/1 mL) and the mixture was heated at 90 °C for 10 min. After cooling to rt, the
11 solution was diluted with HPLC eluent (2.5 mL) and purified by semipreparative HPLC (SiO₂ column;
12 DCM/EtOH/NH₄OH 91.8:8:0.2 v/v/v; t_R = 12.1 min). The solvent was evaporated under reduced
13 pressure and the formulation was achieved in EtOH/saline (05:95; v/v; formulation yield: 93%). [¹⁸F]**9**
14 was obtained in 65 min with 34% overall RCY (25% non-decay-corrected), and a specific activity of
15 81-139 GBq.μmol⁻¹. RCP was determined by analytical HPLC (C18 column; MeOH/H₂O/NH₄OH
16 v/v/v; 59.9:39.9:0.2 to 89.8:10:0.2 linear gradient in 10 min then 59.9:39.9:0.2 isocratic during 7 min;
17 0.9 mL.min⁻¹; t_R = 12.59 min) and was >99%. Color spot test showed no detection of K₂₂₂ in the final
18 injectable [¹⁸F]**9** solution. Radiotracer was radiochemically stable at rt for at least 6 h after preparation.
19 LogD = 0.95±0.02.
20
21
22
23
24
25
26
27
28
29
30
31
32
33
34
35
36
37
38
39
40

41 ACKNOWLEDGMENT We would like to thank the CLARA (Cancéropôle Lyon Rhône-Alpes
42 Auvergne), the Auvergne Regional Council, the Puy de Dôme General Council, Clermont Community,
43 the European Regional Development Fund, the European Union, The French Ligue contre le Cancer and
44 the Bullukian Foundation for their financial support. We also thank Martine Bayle, Laurent Audin,
45 Pierre Labarre (INSERM U 990/Université d'Auvergne) and Raphael Boisgard (CEA/SHFJ, Orsay,
46 France) for technical assistance.
47
48
49
50
51

52 ABBREVIATIONS α-MSH, α-melanocyte-stimulating hormone; EI-MS, electron impact mode mass
53 spectra; ESI-MS, electrospray ionization mass spectra; FDG, fluorodeoxyglucose; MC1R, melanocortin
54 type 1 receptor; MsCl, methanesulfonyl chloride; p.i., post injection; RCP, radiochemical purity; RCY,
55
56
57
58
59
60

1 radiochemical yield; SLNB, sentinel lymph node biopsy; TBDMSCl, *tert*-butyldimethylsilyl chloride;
2 TRT, targeted radionuclide therapy.
3
4
5
6
7
8
9
10
11
12
13
14
15
16
17
18
19
20
21
22
23
24
25
26
27
28
29
30
31
32
33
34
35
36
37
38
39
40
41
42
43
44
45
46
47
48
49
50
51
52
53
54
55
56
57
58
59
60

Figure 1. Chemical structure of **1** (ICF01006),²⁹ **2** (ICF01012),²⁸ and **3**,³⁷ three examples of arylcarboxamides with high affinity for melanin-containing cells, evaluated in clinical or preclinical studies.

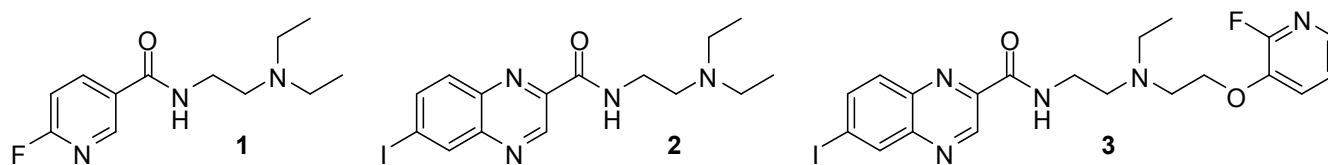
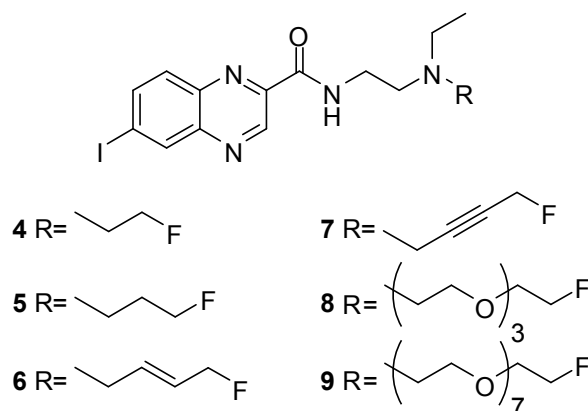
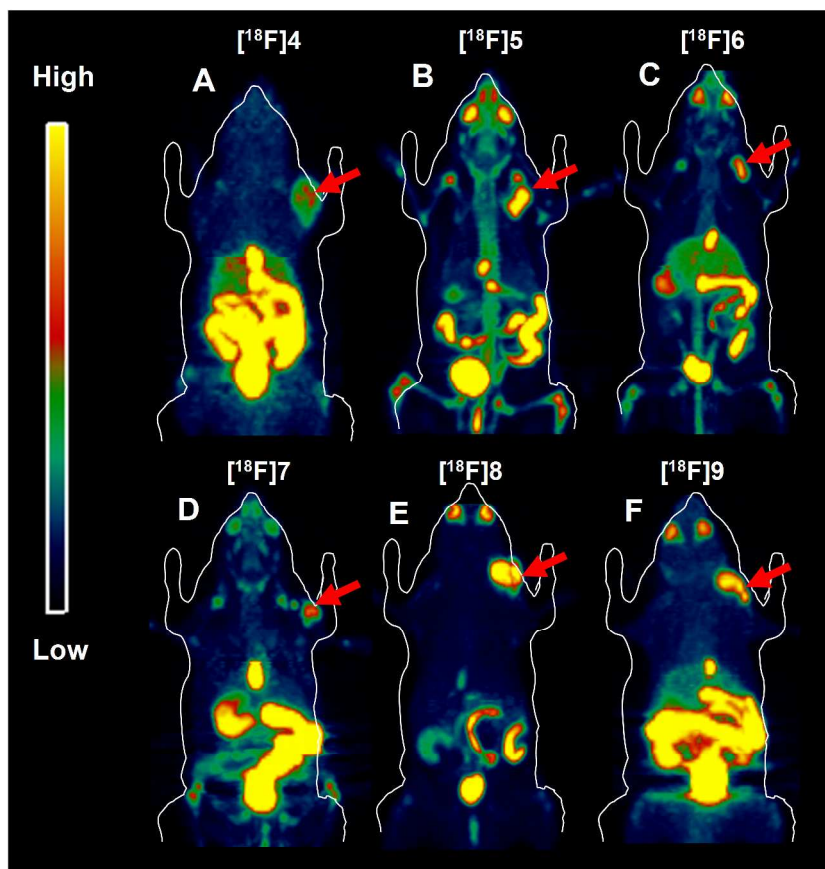


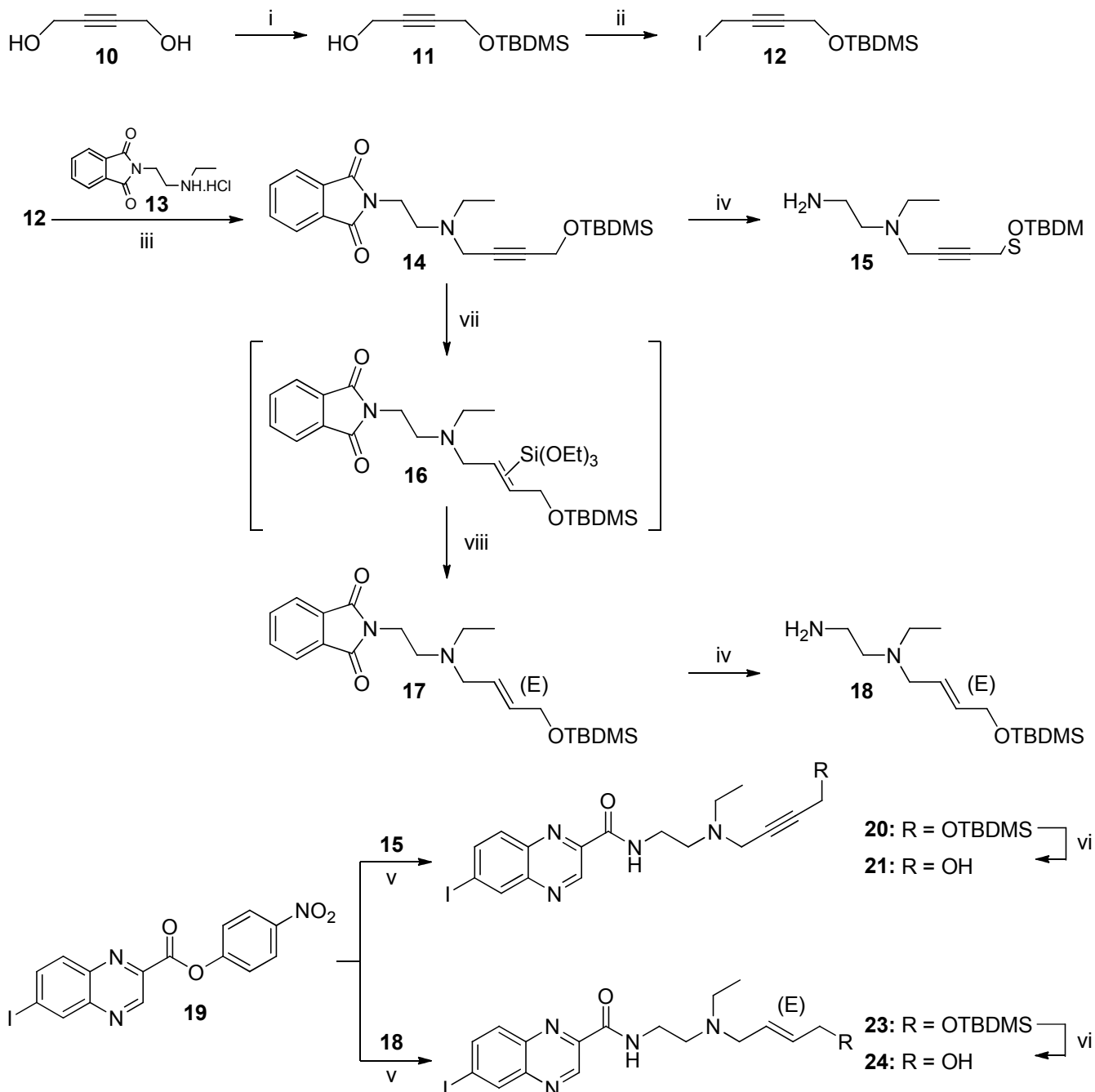
Figure 2. Chemical structures of the six iodinated and fluorinated 6-iodoquinoline-2-carboxamide derivatives investigated.



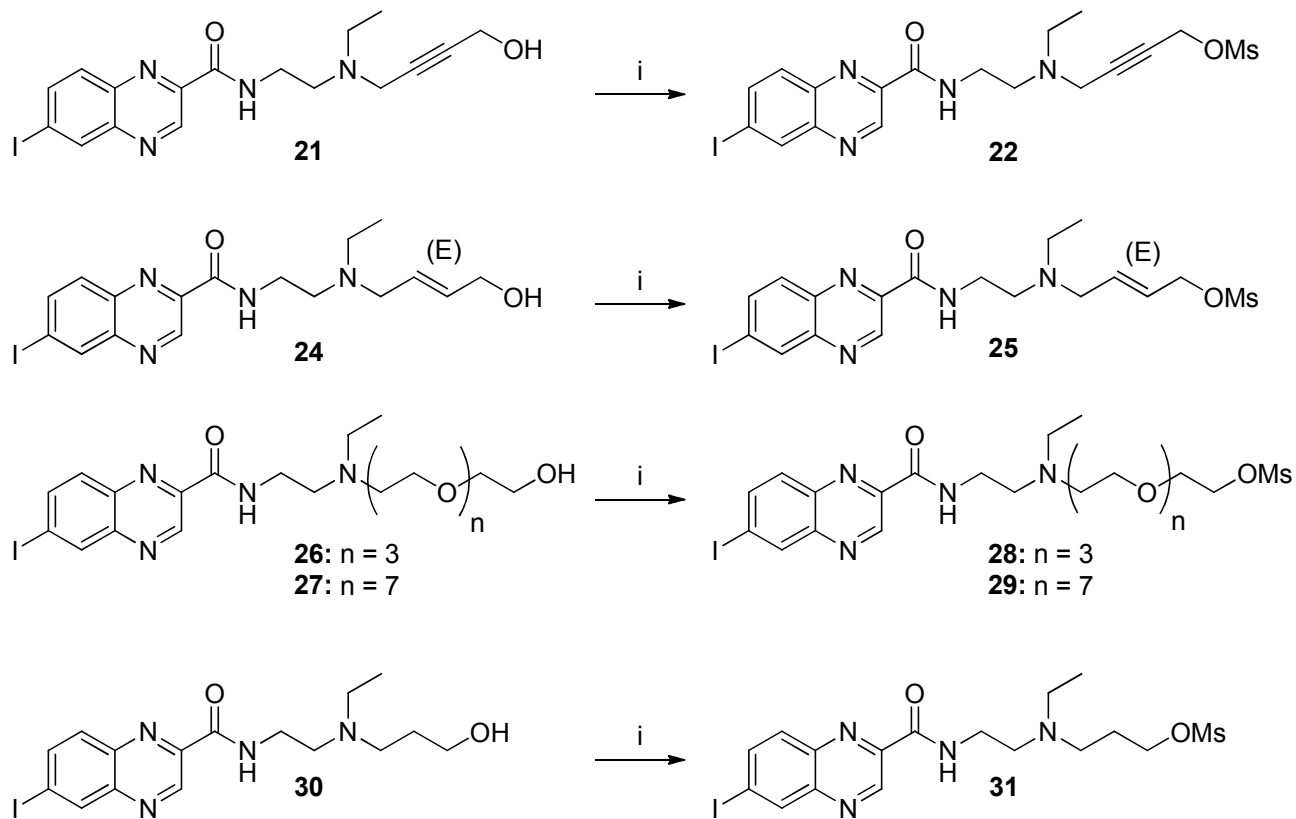
1
2
3
4
5
6
7
8
9
10
11
12
13
14
15
16
17
18
19
20
21
22
23
24
25
26
27
28
29
30
31
32
33
34
35
36
37
38
39
40
41
42
43
44
45
46
47
48
49
50
51
52
53
54
55
56
57
58
59
60

Figure 3. *In vivo* PET imaging biodistribution of radioactivity in B16Bl6 primary melanoma-bearing C57BL/6J mice 1 h after injection of [^{18}F]4 (A), [^{18}F]5 (B), [^{18}F]6 (C), [^{18}F]7 (D), [^{18}F]8 (E) and [^{18}F]9 (F) (8-12 MBq/i.v.). Coronal images represent maximum intensity projections. Tumors are indicated by arrows.

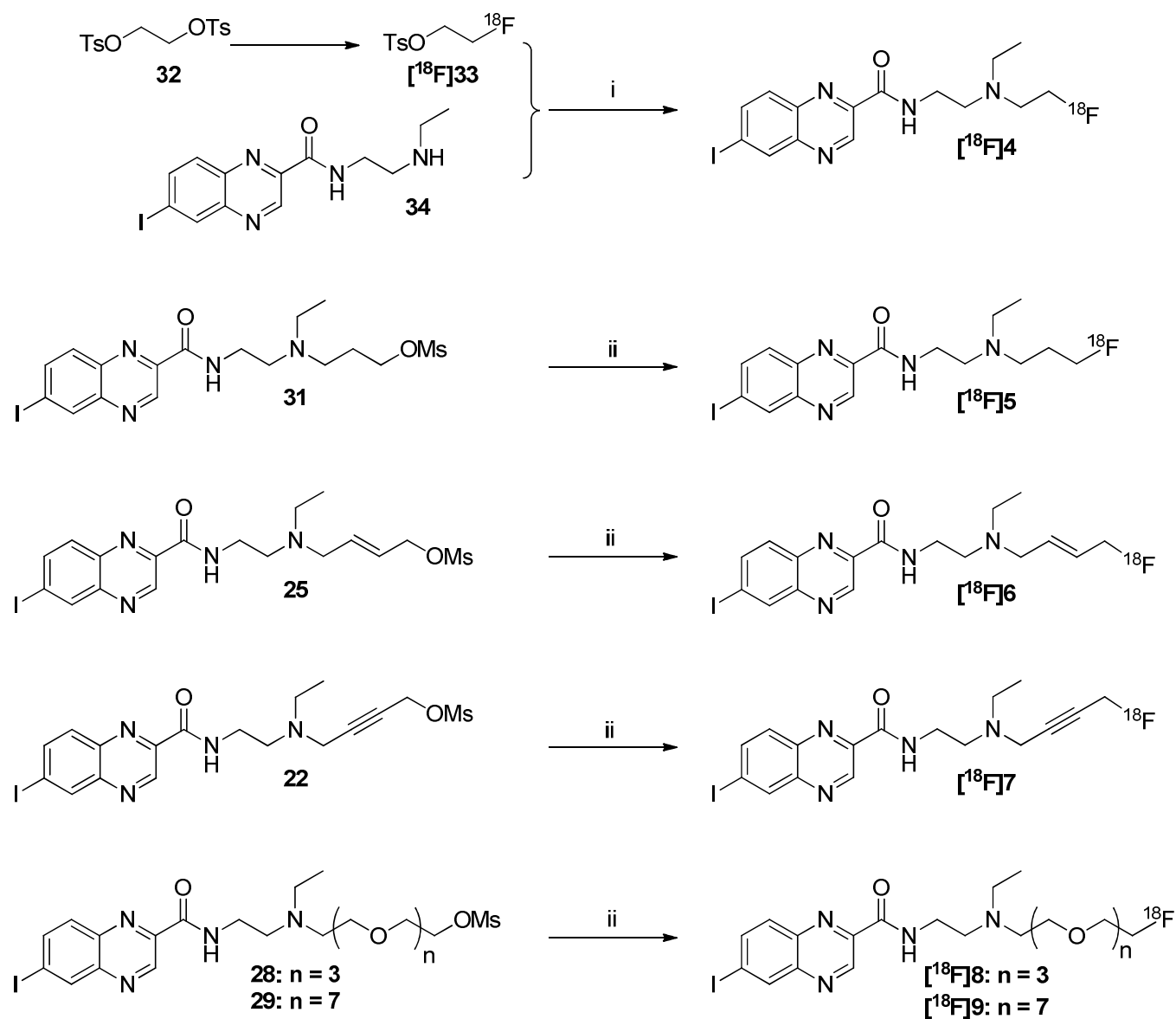


Scheme 1. Syntheses of alcohol **21** and **24**^a

^aReagents and conditions: (i) imidazole, TBDMSCl, DMF, rt, 24 h; (ii) imidazole, PPh₃, I₂, DCM, 0 °C, 30 min, then rt, 1 h; (iii) K₂CO₃, MeCN, rt, 72 h; (iv) NH₂NH₂, H₂O, EtOH, rt, 17 h; (v) THF, rt, 18 h; (vi) TBAF 1M, THF, rt, 2 h; (vii) (EtO)₃SiH, [Cp**Ru*(MeCN)₃]PF₆, DCM, 0 °C, 10 min then rt, 2 h; (viii) AgF 1M in MeOH, THF, rt in darkness, 2.5 h.

Scheme 2. Syntheses of mesylate precursors **22**, **25**, **28**, **29** and **31** required for radiofluorination^a

^aReagents and conditions: (i) MsCl, NEt₃, DMAP, DCM, rt, 30-120 min.

Scheme 3 Radiosyntheses of [^{18}F]4-9^a

^aReagents and conditions: (i) [^{18}F]KF, K_{222} complex, MeCN, 70 °C, 10 min, then 110 °C, 10 min; (ii) [^{18}F]KF, K_{222} complex, MeCN, 90 °C, 10 min.

Table 1. General conditions for [¹⁸F]4-9 radiosyntheses.

Compound	Precursor quantity	Time / temperature	Vessel recovery ^a	HPLC system	Formulation yield ^b	Radiochemical yield ^c	Total synthesis time
[¹⁸ F]4	6+12 mg	10 min/70 °C 10 min/110 °C	67%	SiO ₂ , DCM/EtOH 98:02 v/v	97%	11%	91 min
[¹⁸ F]5	14 mg	10 min/90 °C	87%	SiO ₂ , DCM/EtOH 94:06 in 0.2% NH ₄ OH	91%	54%	70 min
[¹⁸ F]6	12 mg	10 min/90 °C	82%	C18, MeOH/H ₂ O 75:25 in 0.2% NH ₄ OH	83%	16%	62 min
[¹⁸ F]7	10 mg	10 min/90 °C	91%	C18, MeOH/H ₂ O 75:25 in 0.2% NH ₄ OH	76%	22%	59 min
[¹⁸ F]8	13 mg	10 min/90 °C	96%	C18, MeOH/H ₂ O 75:25 in 0.4% NH ₄ OH	90%	21%	57 min
[¹⁸ F]9	15 mg	10 min/90 °C	85%	SiO ₂ , DCM/EtOH 92:08 in 0.2% NH ₄ OH	93%	34%	65 min

^adetermined by measuring the radioactivity in the reactor before and after injection onto HPLC system

^bdetermined by dividing the final amount of radioactivity by the radioactivity measured after HPLC, non decay corrected

^cincluding formulation step, decay corrected

Table 2. PET images quantitative analysis of tumors and major organs at 1 h p.i. of [¹⁸F]4-9 (8-12 MBq/mouse, n=2-5). Data are expressed as percentage of injected dose per gram of tissue (% ID/g)±SD. Means are compared using Student *t* test (p<0.05 is considered statistically significant).

	[¹⁸ F]4	[¹⁸ F]5	[¹⁸ F]6	[¹⁸ F]7	[¹⁸ F]8	[¹⁸ F]9
% ID/g	n=5	n=3	n=2	n=3	n=8	n=3
Tumor	2.02 ± 1.06	10.56 ± 1.76	6.74 ± 0.73	4.16 ± 0.41	14.33 ± 2.11 ^{*†‡□¥}	6.63 ± 1.64
Muscle	1.02 ± 0.26	0.90 ± 0.11	0.83 ± 0.12	0.82 ± 0.04	1.37 ± 0.37	1.01 ± 0.09
Eyes	1.40 ± 0.34	10.46 ± 1.08	9.49 ± 0.34	2.70 ± 0.36	10.50 ± 2.95 ^{*□¥}	5.53 ± 1.35
Bones	1.31 ± 0.01	7.05 ± 0.21 [†]	3.39 ± 0.31 [‡]	2.77 ± 0.47	1.98 ± 0.56	2.48 ± 0.39
Ratios						
TMR^a	1.95 ± 0.69	11.86 ± 2.43	8.27 ± 2.05	5.07 ± 0.32	11.04 ± 2.87 ^{*†□}	6.62 ± 1.90
TBR^b	1.31 ± 0.00	1.50 ± 0.22	1.99 ± 0.03	1.46 ± 0.07	7.65 ± 2.50 ^{*†‡□¥}	2.67 ± 0.49

^aTumor-to-Muscle Ratio ; ^bTumor-to-Bone Ratio

* Comparison of [¹⁸F]8 and [¹⁸F]4

† Comparison of [¹⁸F]8 and [¹⁸F]5

‡ Comparison of [¹⁸F]8 and [¹⁸F]6

□ Comparison of [¹⁸F]8 and [¹⁸F]7

¥ Comparison of [¹⁸F]8 and [¹⁸F]9

Table 3. *Ex vivo* biodistribution of [¹⁸F]8 and [¹⁸F]9 in B16Bl6 primary melanoma-bearing C57BL/6J mice at 1 h, 2 h, and 3 h p.i. Data are expressed as percentage of injected dose per gram of tissue (% ID/g)±SD (n=5-6).

	[¹⁸ F]8			[¹⁸ F]9			
	% ID/g	1 h (n=5)	2 h (n=6)	3 h (n=5)	1 h (n=6)	2 h (n=5)	3 h (n=6)
Tumor		14.05 ± 1.42 [*]	13.07 ± 1.22 [†]	11.55 ± 1.24 [‡]	9.81 ± 2.96	5.81 ± 1.37	6.76 ± 1.35
Muscle		1.17 ± 0.12	0.92 ± 0.15	0.81 ± 0.10 [*]	1.07 ± 0.35	1.04 ± 0.24	1.11 ± 0.34
Eyes		18.36 ± 4.74	18.17 ± 3.15	17.96 ± 2.73	12.24 ± 4.39	12.10 ± 1.85	13.43 ± 2.17
Bones		1.40 ± 0.10	1.96 ± 0.51	3.27 ± 0.70	1.82 ± 0.55	2.13 ± 0.19 [*]	3.61 ± 1.12
Blood		1.42 ± 0.32	1.12 ± 0.24	0.80 ± 0.07	1.15 ± 0.19	1.37 ± 0.30	0.99 ± 0.20
Skin		1.44 ± 0.19	1.51 ± 0.53	1.05 ± 0.12	1.22 ± 0.22	0.94 ± 0.51	1.47 ± 0.49
Liver		2.56 ± 0.22	1.88 ± 0.34	1.99 ± 0.45	2.02 ± 0.19	2.31 ± 0.64	2.60 ± 1.37
Stomach		4.41 ± 1.36	2.48 ± 0.88	2.81 ± 2.23	5.87 ± 3.32	7.35 ± 4.79 [*]	5.39 ± 3.13
Small intestine		7.58 ± 1.80	4.28 ± 1.18	3.91 ± 1.05	16.68 ± 7.93 [*]	19.51 ± 5.43 [‡]	18.62 ± 13.65 [*]
Caecum		7.27 ± 0.62	8.94 ± 1.78	10.79 ± 1.54	6.37 ± 4.84	12.10 ± 10.31	29.31 ± 17.94 [*]
Colon+faeces		7.17 ± 2.93	6.05 ± 1.72	8.09 ± 5.04	7.39 ± 1.36	8.14 ± 1.78 [*]	12.63 ± 7.83
Kidney		3.46 ± 0.53	2.18 ± 0.43	2.19 ± 0.36	3.60 ± 1.74	3.52 ± 1.02	2.60 ± 1.69
Spleen		3.72 ± 1.49 [*]	2.88 ± 2.11	1.87 ± 0.38	2.35 ± 0.91	2.38 ± 0.87	2.35 ± 0.98
Pancreas		2.09 ± 0.42	1.33 ± 0.28	1.33 ± 0.35	2.63 ± 1.33	1.56 ± 0.38	1.81 ± 0.66
Lung		1.86 ± 0.15	1.65 ± 0.11	1.60 ± 0.09	1.75 ± 0.18	1.72 ± 0.72	2.37 ± 0.67 [*]
Heart		2.72 ± 0.18	2.14 ± 0.33	2.32 ± 0.50	1.58 ± 0.24	1.70 ± 0.24	3.00 ± 1.12
Brain		1.82 ± 0.08 [*]	1.39 ± 0.25	1.37 ± 0.35	1.03 ± 0.18	1.03 ± 0.10	1.72 ± 0.67
Ratio							
TMR^a		12.12 ± 2.29 [*]	14.46 ± 2.62 [‡]	14.46 ± 3.06 [‡]	9.48 ± 2.41	5.75 ± 1.45	6.64 ± 2.69
TBR^b		10.24 ± 2.83	12.19 ± 3.32 [†]	14.43 ± 1.75 [‡]	8.29 ± 2.87	4.01 ± 1.12	5.27 ± 0.20
TBoR^c		10.11 ± 1.87 [‡]	7.13 ± 2.21 [‡]	3.70 ± 1.17 [*]	5.35 ± 0.82	2.75 ± 0.80	2.16 ± 1.15

^aTumor-to-Muscle Ratio; ^bTumor-to-Blood Ratio; ^cTumor-to-Bone Ratio

^{*} p<0.05, [†] p<0.01, [‡] p<0.001 as determined by Student *t* test

Table 4. *In vivo* stability study of [^{18}F]8 in C57BL/6J mice bearing B16 murine melanoma. Results are expressed as percentage of unchanged [^{18}F]8 relative to total radioactivity signal.

Unchanged [^{18}F]8	1 h	2 h
Blood	15% ^a	n.d. ^b
Tumor	>99%	>99%
Eyes	>99%	>99%
Liver	8%	n.d. ^b
Urines	0.1%	n.d. ^b

^aat 30 min; ^bnot detectable

1
2
3 REFERENCES
4
5
6
7
8
9
10
11
12
13
14
15
16
17
18
19
20
21
22
23
24
25
26
27
28
29
30
31
32
33
34
35
36
37
38
39
40
41
42
43
44
45
46
47
48
49
50
51
52
53
54
55
56
57
58
59
60

1. Garbe, C.; Peris, K.; Hauschild, A.; Saiag, P.; Middleton, M.; Spatz, A.; Grob, J. J.; Malvehy, J.; Newton-Bishop, J.; Stratigos, A.; Pehamberger, H.; Eggermont A. Diagnosis and treatment of melanoma: European consensus-based interdisciplinary guideline. *Eur. J. Cancer* **2010**, *46*, 270–283.
2. Garbe, C.; Leiter, U. Melanoma epidemiology and trends. *Clin. Dermatol.* **2009**, *27*, 3–9.
3. Jennings, L.; Murphy, G. M. Predicting outcome in melanoma: where are we now? *Br. J. Dermatol.* **2009**, *16*, 496–503.
4. Balch, C. M.; Gershenwald, J. E.; Soong, S. J.; Thompson, J. F.; Atkins, M. B.; Byrd, D. R.; Buzaid, A. C.; Cochran, A. J.; Coit, D. G.; Ding, S.; Eggermont, A. M.; Flaherty, K. T.; Gimotty, P. A.; Kirkwood, J. M.; McMasters, K. M.; Mihm, M. C. Jr.; Morton, D. L.; Ross, M. I.; Sober, A. J.; Sondak, V. K. final version of 2009 AJCC melanoma staging and classification. *J. Clin. Oncol.* **2009**, *27*, 6199–6206.
5. Scott, J. D.; McKinley, B. P.; Bishop, A.; Trocha, S. D. Treatment and outcomes of melanoma with a Breslow's depth greater than or equal to one millimeter in a regional teaching hospital. *Am. Surg.* **2005**, *71*, 198–201.
6. Phan, G. Q.; Messina J. L.; Sondak, V. K.; Zager, J. S. Sentinel lymph node biopsy for melanoma: indications and rationale. *Cancer Control.* **2009**, *16*, 234–239.
7. Garbe, C.; Eigentler, T. K.; Keilholz, U.; Hauschild, A.; Kirkwood, J. M. Systematic review of medical treatment in melanoma: current status and future prospects. *Oncologist* **2011**, *16*, 5–24.
8. Tarhini, A. A.; Agarwala, S. S. Cutaneous melanoma: available therapy for metastatic disease. *Dermatol. Ther.* **2006**, *19*, 19–25.
9. Garbe, C.; Eigentler, T. K. Diagnosis and treatment of cutaneous melanoma: state of the art 2006. *Melanoma Res.* **2007**, *17*, 117–127.
10. Punt, C. J.; Suci, S.; Gore, M. A.; Koller, J.; Kruit, W. H.; Thomas, J.; Patel, P.; Lienard, D.; Eggermont, A. M.; Keilholz, U. Chemoimmunotherapy with dacarbazine, cisplatin, interferon-alpha2b and interleukin-2 versus two cycles of dacarbazine followed by chemoimmunotherapy

- 1
2
3
4
5
6
7
8
9
10
11
12
13
14
15
16
17
18
19
20
21
22
23
24
25
26
27
28
29
30
31
32
33
34
35
36
37
38
39
40
41
42
43
44
45
46
47
48
49
50
51
52
53
54
55
56
57
58
59
60
- in patients with metastatic melanoma: a randomised phase II study of the European Organization for Research and Treatment of Cancer Melanoma Group. *Eur. J. Cancer* **2006**, *42*, 2991–2995.
11. O'Day, S.; Pavlick, A.; Loquai, C.; Lawson, D.; Gutzmer, R.; Richards, J.; Schadendorf, D.; Thompson, J. A.; Gonzalez, R.; Trefzer, U.; Mohr, P.; Ottensmeier, C.; Chao, D.; Zhong, B.; de Boer, C. J.; Uhlir, C.; Marshall, D.; Gore, M. E.; Lang, Z.; Hait, W.; Ho, P. A randomised, phase II study of intetumumab, an anti- α v-integrin mAb, alone and with dacarbazine in stage IV melanoma. *Br. J. Cancer* **2011**, *105*, 346–352.
12. Attia, P.; Phan, G. Q.; Maker, A. V.; Robinson, M. R.; Quezado, M. M.; Yang, J. C.; Sherry, R. M.; Topalian, S. L.; Kammula, U. S.; Royal, R. E.; Restifo, N. P.; Haworth, L. R.; Levy, C.; Mavroukakis, S. A.; Nichol, G.; Yellin, M. J.; Rosenberg, S. A. Autoimmunity correlates with tumor regression in patients with metastatic melanoma treated with anti-CTLA4. *J. Clin. Oncol.* **2005**, *23*, 6043–6053.
13. Chapman, P. B.; Hauschild, A.; Robert, C.; Haanen, J. B.; Ascierto, P.; Larkin, J.; Dummer, R.; Garbe, C.; Testori, A.; Maio, M.; Hogg, D.; Lorigan, P.; Lebbe, C.; Jouary, T.; Schadendorf, D.; Ribas, A.; O'Day, S. J.; Sosman, J. A.; Kirkwood, J. M.; Eggermont, A. M. M.; Dreno, B.; Nolop, K.; Li, J.; Nelson, B.; Hou, J.; Lee, R. J.; Flaherty, K. T.; McArthur, G. A. Improved survival with vemurafenib in melanoma with BRAF V600E mutation. *N. Engl. J. Med.* **2011**, *364*, 2507–2516.
14. Xing, Y.; Cromwell, K. D.; Cormier, J. N. Review of diagnostic imaging modalities for the surveillance of melanoma patients. *Dermatol. Res. Pract.* **2012**, 941921.
15. Krug, B.; Crott, R.; Lonneux, M.; Baurain, J. F.; Pirson, A. S.; Vander Borgh, T. Role of PET in the initial staging of cutaneous malignant melanoma: systematic review. *Radiology* **2008**, *249*, 836–844.
16. Veit-Haibach, P.; Vogt, F. M.; Jablonka, R.; Kuehl, H.; Bockisch, A.; Beyer, T.; Dahmen, G.; Rosenbaum, S.; Antoch, G. Diagnostic accuracy of contrast-enhanced FDG-PET/CT in primary staging of cutaneous malignant melanoma. *Eur. J. Nucl. Med. Mol. Imaging* **2009**, *36*, 910–918.
17. Mirk, P.; Treglia, G.; Salsano, M.; Basile, P.; Giordano, A.; Bonomo, L. Comparison between ^{18}F -Fluorodeoxyglucose positron emission tomography and sentinel lymph node biopsy for regional lymph nodal staging in patients with melanoma: a review of the literature. *Radiol. Res. Pract.* **2011**, 912504.

- 1
2
3
4
5
6
7
8
9
10
11
12
13
14
15
16
17
18
19
20
21
22
23
24
25
26
27
28
29
30
31
32
33
34
35
36
37
38
39
40
41
42
43
44
45
46
47
48
49
50
51
52
53
54
55
56
57
58
59
60
18. Jiménez-Requena, F.; Delgado-Bolton, R. C.; Fernandez-Pérez, C.; Gambhir, S. S.; Schwimmer, J.; Pérez-Vasquez, J. M.; Carreras-Delgado, J. L. Meta-analysis of the performance of ^{18}F -FDG PET in cutaneous melanoma. *Eur. J. Nucl. Med. Mol. Imaging* **2010**, *37*, 284–300.
 19. Wagner, T.; Meyer, N.; Zerdoud, S.; Julian, A.; Chevreau, C.; Payoux, P.; Courbon, F. Fluorodeoxyglucose positron emission tomography fails to detect distant metastases at initial staging of melanoma patients with metastatic involvement of sentinel lymph node. *Br. J. Dermatol.* **2011**, *164*, 1235–1240.
 20. Minn, H.; Vihinen, P. Melanoma imaging with highly specific PET probes: ready for prime time? *J. Nucl. Med.* **2011**, *52*, 5–7.
 21. Sturm, R. A. Skin colour and skin cancer - MC1R, the genetic link. *Melanoma Res.* **2002**, *12*, 405–416.
 22. Miao, Y.; Whitener, D.; Feng, W.; Owen, N. K.; Chen, J.; Quinn, T. P. Evaluation of the human melanoma targeting properties of radiolabeled alpha-melanocyte stimulating hormone peptide analogues. *Bioconjugate Chem.* **2003**, *14*, 1177–1184.
 23. Guo, H.; Shenoy, N.; Gershman, B. M.; Yang, J.; Sklar, L. A.; Miao, Y. Metastatic melanoma imaging with an ^{111}In -labeled lactam bridge-cyclized alpha-melanocyte stimulating hormone peptide. *Nucl. Med. Biol.* **2009**, *36*, 267–276.
 24. Cheng, Z.; Zhang, L.; Graves, E.; Xiong, Z.; Dandekar, M.; Chen, X.; Gambhir, S. S. Small-animal PET of melanocortin 1 receptor expression using a ^{18}F -labeled alpha-melanocyte-stimulating hormone analog. *J. Nucl. Med.* **2007**, *48*, 987–994.
 25. Ren, G.; Liu, Z.; Miao, Z.; Liu, H.; Subbarayan, M.; Chin, F. T.; Zhang, L.; Gambhir, S. S.; Cheng, Z. PET of Malignant melanoma using labeled metalloptides. *J. Nucl. Med.* **2009**, *50*, 1865–1872.
 26. Ren, G.; Liu, S.; Liu, H.; Miao, Z.; Cheng, Z. Radiofluorinated rhenium cyclized α -MSH analogues for PET imaging of melanocortin receptor 1. *Bioconjugate Chem.* **2010**, *21*, 2355–2360.
 27. Eisenhut, M.; Hull, W. E.; Mohammed, A.; Mier, W.; Lay, D.; Just, W.; Gorgas, K.; Lehmann, W. D.; Haberkorn, U. Radioiodinated N-(2-diethylaminoethyl)benzamide derivatives with high melanoma uptake: structure-affinity relationships, metabolic fate, and intracellular localization. *J. Med. Chem.* **2000**, *43*, 3913–3922.

- 1
2
3
4
5
6
7
8
9
10
11
12
13
14
15
16
17
18
19
20
21
22
23
24
25
26
27
28
29
30
31
32
33
34
35
36
37
38
39
40
41
42
43
44
45
46
47
48
49
50
51
52
53
54
55
56
57
58
59
60
28. Chezal, J. M.; Papon, J.; Labarre, P.; Lartigue, C.; Galmier, M. J.; Decombat, C.; Chavignon, O.; Maublant, J.; Teulade, J. C.; Madelmont, J. C.; Moins, N. Evaluation of radiolabeled (hetero)aromatic analogues of N-(2-diethylaminoethyl)-4-iodobenzamide for imaging and targeted radionuclide therapy of melanoma. *J. Med. Chem.* **2008**, *51*, 3133–3144.
29. Madelmont, J. C.; Chezal, J. M.; Moins, N.; Teulade, J. C.; Chavignon, O. Labeled analogues of halobenzamides as radiopharmaceuticals. World Patent WO2008012782, 2008.
30. Greguric, I.; Taylor, S. R.; Denoyer, D.; Ballantyne, P.; Berghofer, P.; Roselt, P.; Pham, T. Q.; Mattner, F.; Bourdier, T.; Neels, O. C.; Dorow, D. S.; Loc'h, C.; Hicks, R. J.; Katsifis, A. Discovery of [^{18}F]N-(2-(diethylamino)ethyl)-6-fluoronicotinamide: a melanoma positron emission tomography imaging radiotracer with high tumour to body contrast ratio and rapid renal clearance. *J. Med. Chem.* **2009**, *52*, 5299–5302.
31. Denoyer, D.; Greguric, I.; Roselt, P.; Neels, O. C.; Aide, N.; Taylor, S. R.; Katsifis, A.; Dorow, D. S.; Hicks, R. J. High-contrast PET of melanoma using [^{18}F]MEL050, a selective probe for melanin with predominantly renal clearance. *J. Nucl. Med.* **2010**, *51*, 441–447.
32. Rbah-Vidal, L.; Vidal, A.; Besse, S.; Cachin, F.; Bonnet M.; Audin L.; Askienazy S.; Dollé F.; Degoul F.; Miot-Noirault E.; Moins N.; Auzeloux P.; Chezal, J. M. Early detection and longitudinal monitoring of experimental primary and disseminated melanoma using [^{18}F]ICF01006, a highly promising melanoma PET tracer. *Eur. J. Nucl. Med. Mol. Imaging* **2012**, *39*, 1449–1461.
33. Bonnet-Duquennoy, M.; Papon, J.; Mishellany, F.; Labarre, P.; Guerquin-Kern, J. L.; Wu, T. D.; Gardette, M.; Maublant, J.; Penault-Llorca, F.; Miot-Noirault, E.; Cayre, A.; Madelmont, J. C.; Chezal, J. M.; Moins, N. Targeted radionuclide therapy of melanoma: Anti-tumoural efficacy studies of a new ^{131}I labelled potential agent. *Int. J. Cancer* **2009**, *125*, 708–716.
34. Bonnet, M.; Mishellany, F.; Papon, J.; Cayre, A.; Penault-Llorca, F.; Madelmont, J. C.; Miot-Noirault, E.; Chezal, J. M.; Moins, N. Anti-melanoma efficacy of internal radionuclide therapy in relation to melanin target distribution. *Pigment Cell Melanoma Res.* **2010**, *23*, e1–e11.
35. Boisgard, R.; Chezal, J. M.; Dollé, F.; Kuhnast, B.; Madelmont, J. C.; Maisonial, A.; Miot-Noirault, E.; Moins, N.; Papon, J.; Tavitian, B. Labelled analogues of halobenzamides as multimodal radiopharmaceuticals and their precursors. World Patent WO2009095872, 2009.

- 1
2
3
4
5
6
7
8
9
10
11
12
13
14
15
16
17
18
19
20
21
22
23
24
25
26
27
28
29
30
31
32
33
34
35
36
37
38
39
40
41
42
43
44
45
46
47
48
49
50
51
52
53
54
55
56
57
58
59
60
36. Auzeloux, P.; Billaud, E. M. F.; Chezal, J. M.; Madelmont, J. C.; Maisonial, A.; Miot-Noirault, E.; Papon, J.; Rbah-Vidal, L.; Vidal, A. Labelled quinoxaline derivatives as multimodal radiopharmaceuticals and their precursors. PCT/IB2013/053106, 2013.
37. Maisonial, A.; Kuhnast, B.; Papon, J.; Boisgard, R.; Bayle, M.; Vidal, A.; Auzeloux, P.; Rbah, L.; Bonnet-Duquennoy, M.; Miot-Noirault, E.; Galmier, M. J.; Borel, M.; Askienazy, S.; Dollé, F.; Tavitian, B.; Madelmont, J. C.; Moins, N.; Chezal, J. M. Single photon emission computed tomography/positron emission tomography imaging and targeted radionuclide therapy of melanoma: new multimodal fluorinated and iodinated radiotracers. *J. Med. Chem.* **2011**, *54*, 2745–2766.
38. Maisonial, A.; Billaud, E. M. F.; Besse, S.; Rbah-Vidal, L.; Papon, J.; Audin, L.; Bayle, M.; Galmier, M. J.; Tarrit, S.; Borel, M.; Askienazy, S.; Madelmont, J.C.; Moins, M.; Auzeloux, P.; Miot-Noirault, E.; Chezal J. M. Synthesis, radioiodination and *in vivo* screening of novel potent iodinated and fluorinated radiotracers as melanoma imaging and therapeutic probes. *Eur. J. Med. Chem.* **2013**, *63*, 840–853.
39. Cai, G.; Zhu, W.; Ma, D. Sequential reaction process to assemble polysubstituted indolizidines, quinolizidines and quinolizidine analogues. *Tetrahedron* **2006**, *62*, 5697–5708.
40. Jones, J. H.; Holtz, W. J.; Edward, J.; Cragoe, E. J., Jr. 6-Substituted 5-chloro-1,3-dihydro-2H-imidazo[4,5-b]pyrazin-2-ones with hypotensive activity. *J. Med. Chem.* **1973**, *16*, 537–542.
41. Denoyer, D.; Labarre, P.; Papon, J.; Miot-Noirault, E.; Galmier, M.J.; Madelmont, J.C.; Chezal, J.M.; Moins, N. Development of a high-performance liquid chromatographic method for the determination of a new potent radioiodinated melanoma imaging and therapeutic agent. *J. Chromatogr., B: Anal. Technol. Biomed. Life Sci.* **2008**, *875*, 411–418.
42. Trost, B. M.; Ball, Z. T.; Joege, T. A chemoselective reduction of alkynes to (E)-alkenes. *J. Am. Chem. Soc.* **2002**, *124*, 7922–7923.
43. Fürstner, A.; Radkowski, K. A chemo- and stereoselective reduction of cycloalkynes to (E)-cycloalkenes. *Chem. Commun.* **2002**, 2182–2183.
44. Hara, T.; Kosaka, N.; Kishi, H. Development of ¹⁸F-fluoroethylcholine for cancer imaging with PET: synthesis, biochemistry, and prostate cancer imaging. *J. Nucl. Med.* **2002**, *43*, 187–199.

- 1
2
3
4
5
6
7
8
9
10
11
12
13
14
15
16
17
18
19
20
21
22
23
24
25
26
27
28
29
30
31
32
33
34
35
36
37
38
39
40
41
42
43
44
45
46
47
48
49
50
51
52
53
54
55
56
57
58
59
60
45. Wester, H. J.; Herz, M.; Weber, W.; Heiss, P.; Senekowitsch-Schmidtke, R.; Schwaiger, M.; Stöcklin, G. Synthesis and radiopharmacology of *O*-(2-[¹⁸F]fluoroethyl)-L-tyrosine for tumour imaging. *J. Nucl. Med.* **1999**, *40*, 205–212.
46. Armarego, W. L. F.; Perrin, D. D. Purification of laboratory chemicals. 4th ed.; Butterworth-Heinemann Eds.; reed educational and professional Publishing Ltd: Oxford, **1996**
47. Mock, B. H.; Winkle, W.; Vavrek, M. T. A color spot test for the detection of Kryptofix 2.2.2 in [¹⁸F]FDG preparations. *Nucl. Med. Biol.* **1997**, *24*, 193–195.
48. Wang, Y.; Seidel, J.; Tsui, B. M. W.; Vaquero, J. J.; Pomper, M. G. Performance evaluation of GE healthcare eXplore VISTA dual-ring small-animal PET scanner. *J. Nucl. Med.* **2006**, *47*, 1891–1900.

Table Of Contents.

